A TORTUOSITY-DRIVEN MICROFLUIDIC THROMBOSIS AND HEMOSTASIS MONITORING DEVICE APPLIED IN A PEDIATRIC CRITICAL CARE UNIT

A Thesis

by

DAVID JORDAN LUNA

Submitted to the Office of Graduate and Professional Studies of
Texas A&M University
in partial fulfillment of the requirements for the degree of

MASTER OF SCIENCE

Chair of Committee,	Abhishek Jain
Committee Members,	Saurabh Biswas
	Victor Ugaz
	Egemen Tuzun
Head of Department,	Michael J. McShane

August 2019

Major Subject: Biomedical Engineering

ABSTRACT

Bleeding and thrombosis episodes in children are often encountered during ECMO/VAD. Pediatric patients on ECMO are known to have compromised platelet function and depleted plasma factors, making them susceptible to bleeding when anticoagulated with heparin. More concerning is the fact that hematology tests (ACT, aPTT, Anti-Xa) often report positive even when bleeding risk is present. TEG and ROTEM do provide greater information about whole blood coagulation, however a major deficiency with these tests is that they measure clotting characteristics under conditions that are not physiologically-relevant, thus limiting their ability to assess platelet function. To overcome these limitations, we developed a rapid and ultra-low volume tortuosity-activated microfluidic device for whole blood coagulation monitoring in pediatric critical care patients.

The microfluidic device contains channels made of soft lithography that mimics a stenosed arteriolar blood vessel network and incorporates bio-rheological parameters known to induce clot formation such as blood vessel tortuosity and shear gradients. When the device is connected to a pressure sensor and whole blood is perfused it provides a tool to quantitatively determine clotting time. We demonstrate that the clotting times increase when clinically-relevant doses of heparin and bivalirudin is added to healthy blood samples. In addition, we validate these measurements by showing fluorescent images of that fibrin inhibition. Furthermore, we found that the clotting times were similar for devices coated with rat or human collagen, yet significantly different for horse collagen

treated devices. Also, we saw that clotting time is dependent on platelet count. Lastly, we did not measure any microchannel occlusion when the device was treated with blood from pediatric ECMO patients. We then found that this lack of occlusion is due to poor platelet adhesion. We test if platelet adhesion can be restored with the addition of von willebrand factor (VWF).

DEDICATION

To my grandparents Louis Mendoza, Margarita Mendoza, "Mama" Lupe Luna, and José Antonio Luna

ACKNOWLEDGEMENTS

I would like to acknowledge for my family, mentors, and friends for their support and encouragement.

I want to especially thank my colleagues in Dr. Abhishek Jain's Bioinspired Translational Microsystems laboratory for their friendship and guidance.

Lastly, I would like to thank Dr. Abhishek Jain for his mentorship.

CONTRIBUTORS AND FUNDING SOURCES

Contributors

This work was supervised by a dissertation committee consisting of Professor Abhishek Jain (advisor) and Professors Saurabh Biswas and Egemen Tuzun of the Department of Biomedical Engineering and Professor Victor Ugaz of the Department of Chemical Engineering.

All other work conducted for the dissertation was completed by the student independently.

Funding Sources

This work was funded by Texas A&M Engineering Experiment Station and Baylor College of Medicine. Its contents are solely the responsibility of the authors and do not necessarily represent the official views of the TEES or BCM.

NOMENCLATURE

ACT	Activated Clotting Time
aPTT	Activated Partial Thromboplastin Time
TEG	Thromboelastography
ROTEM	Rotational Thromboelastography
ECLS	Extracorporeal Life Support
ECMO	Extracorporeal Membrane Oxygenation
VAD	Ventricular Assist Device
VWF	Von Willebrand Factor
PPP	Platelet Poor Plasma
CFD	Computational Fluid Dynamics
UFH	Unfractionated Heparin
PDMS	Polydimethylsiloxane
TCMS	Tri-Chloro-Methyl-Silane

TABLE OF CONTENTS

Page

LIST OF FIGURES

Page

LIST OF TABLES

Page

1. INTRODUCTION

1.1 Overview of Hemostasis Monitoring in Pediatric Extracorporeal Life Support

Hemostasis monitoring is critically important in pediatric patients on extracorporeal life support systems (ECLS) and receiving anticoagulant and anti-platelet therapies to anticipate, avoid and direct the management of bleeding and thrombotic risk [1-3]. However, despite routine monitoring bleeding still occurs in ~70% of pediatric patients on extracorporeal life support (ECMO) and is independently associated with higher daily risk of mortality [4]. This high bleeding occurrence is partly due to the fact that the coagulation tests (activated clotting time, activated partial thromboplastin time, Anti-Xa) used for unfractionated heparin monitoring lack specificity and sensitivity and often result in false positive or negative cases in the clinic, thus providing misleading information about a patient's coagulation status [5-7]. Also, the results produced by these assays can vary considerably depending on sample preparation, addition of activators, equipment, and user expertise. Moreover, these tests do not provide information on platelet function, further limiting their ability to predict bleeding and thrombotic risk.

Because of the limitations of conventional coagulation tests, new point-of-care monitoring systems, such as thromboelastography (TEG) and rotational thromboelastography (ROTEM) devices have been integrated into pediatric clinical laboratories. These devices are able to provide greater information about whole blood coagulation because they measure the cumulative contributions of plasma, platelets, leukocytes and red blood cells

to the clotting response. These tests, however, measure clotting characteristics under static conditions (no flow) and hence, they are limited in their clinical utility with respect to platelet and endothelial cell functions, which are highly sensitive to physical forces, including pressure and flow [8]. For example, fluid shear stresses and gradients of shear stresses in blood have a major impact on platelet activation and thrombosis and thus, coagulation monitors that do not incorporate fluid dynamics fail to accurately assess blood coagulation physiology as it occurs in the vasculature of a living patient [9, 10].

To address these limitations, a biomimetic microfluidic whole blood coagulation monitoring medical device was designed to mimic a network of stenosed arteriole blood vessels and incorporate relevant hemodynamic mechanical cues (shear stress and gradients) [11]. This biomimetic system was demonstrated to have several advantages over current coagulation tests. For example, whole blood tests could be carried out with minimal (or none) sample preparation or operator training, *in vitro* or *ex vivo*, and integrated with extracorporeal blood perfusion systems. But this system takes more than 1 mL of blood and in some cases and requires more than 15 minutes to complete analysis. Therefore, despite being biomimetic, it may not be very versatile for many lab-on-a-chip applications, particularly in neonatal and pediatric care, where rapid analysis with minimal amount of blood use is required.

To further innovate the coagulation monitor, we have invented a biomimetic, rapid and ultra-low-volume whole blood thrombosis and hemostasis monitoring system. Tortuous

vessels have been shown to induce fluid dynamical disturbances and shear gradients that make them hotspots for forming thrombi *in vivo* [12]. Also, some prior studies have shown increased thrombosis due to tortuosity *in vitro* [13]. Hence, we harnessed these biological architectural principles and created a device with the integration of shear-gradients caused by tortuosity to stenosis-like expansion-contractions in the microfluidic format. We found this newly designed assay requires less than 1mL of blood and takes less than 15 minutes to complete when tested with pediatric blood samples.

1.1.1 Tests to Measure Anticoagulant Effect on Coagulation Status

This section will describe the different tests used to monitor unfractionated heparin therapy (UHF) in pediatric ECLS:

In general, there are three major limitations associated with current UHF monitoring tests. The first is that these tests fail to incorporate the effects of the endothelium in its assessment of coagulation status. The second limitation is that the majority of these tests are plasma-based tests, providing partial functional measures of coagulation, and not whole blood tests that incorporate platelet function and assessment of clot strength. Lastly, there lacks test standardization.

1.1.1.1 Activated Clotting Time (ACT)

The activated clotting time (ACT) is an inexpensive point of care whole blood test. ACT measures the time in seconds of whole blood to form fibrin clot after the addition of various coagulation activator [14]. ACT does not measure clot strength. A limitation of the is that ACT results will vary based on many factors including platelet number and function, fibrinogen level, coagulation factor deficiencies, patient temperature, hemodilution, and technical factors. Hence, it does not represent, solely, UFH effect. Baird and colleagues retrospectively reviewed over 600 pediatric ECMO patients and found only a modest correlation ($r = 0.48$) between ACT and UFH dose suggesting that ACT is not an accurate tool for monitoring UFH anticoagulation during pediatric ECMO [5].

1.1.1.2 Activated Partial Thromboplastin Time (aPPT)

The aPTT is a plasma-based test that measures the time from Factor XII activation to fibrin formation, after addition of calcium and a reagent. The aPTT guidelines were developed based on data from adults [15]. These guidelines suggest that an aPTT between 1.5 and 2.5x the patient's pre-therapy baseline is normal. However, the baseline aPTT in sick pediatric patients is very different from normal adult controls, which limits the utility of aPTT as a measure of UFH effect. Hence, there is a high degree of intra- and interpatient variability especially in infants [6].

1.1.1.3 Anti-Xa Assay

The anti-Xa assay (alternatively called the heparin level) is a measure of UFH effect based on the ability of UFH to catalyze AT's inhibition of Factor Xa. Anti-Xa is a plasma-based test that does not incorporate platelet function [16]. The anti-Xa assay evaluates only one chemical reaction of the UFH–AT complex; it does not measure inhibition of thrombin. The anti-Xa is used as a surrogate measure of the overall anticoagulant activity of UFH. The same adult study that set the therapeutic aPTT at 1.5–2.5x the patient's baseline aPTT demonstrated that this therapeutic aPTT range corresponded to an anti-Xa activity of 0.3–0.7 U/mL. A few single-center ECLS case series have found an improved association of anti-Xa with UFH dose and decreased blood sampling, decrease in blood product transfusion, and less complications, both thrombotic and hemorrhagic [17].

1.1.1.4 Viscoelastic testing

Viscoelastic tests [thromboelastography (TEG) and rotational thromboelastometry (ROTEM)] examine whole blood clot formation (coagulation) and dissolution (fibrinolysis). They are limited by static conditions (no flow) as well as the exclusion of vascular endothelium, but they are the only option available to evaluate clot strength. Additional benefits include POC testing that can be performed at the bedside and at the patient's temperature. Additional information from viscoelastic testing includes time until initial fibrin formation, the kinetics of fibrin formation and clot development, the ultimate strength and stability of the fibrin clot, clot lysis, and platelet function [18]. TEG and ROTEM are not yet widely available; only 43% of centers use viscoelastic tests as part of

their routine anticoagulation monitoring on ECLS**.** There are limited reports documenting improved outcomes when TEG was incorporated into a bundled anticoagulation protocol [19].

1.1.2 Tests to Measure Platelet Function

This section will describe that different tests used to measure platelet function in pediatric ECLS:

In general, there are two major limitations associated with current platelet function tests. The first is that these tests fail to incorporate the effects of the endothelium in its assessment of platelet function. The second limitation is that the majority of these tests are platelet rich plasma tests, providing partial functional measures of platelet function, and not whole blood tests that incorporate the effects of other cellular components and assessment of clot strength.

1.1.2.1 Platelet Aggregometry

Platelet aggregometry is a primary hemostasis test. It is considered to be the gold standard for platelet function assays [20]. According to a recent international survey, 93% laboratories use platelet-rich plasma (PRP), and 7% laboratories use whole blood [21]. Whole blood assays have the advantage of requiring less specimen volume than PRP methods and is less time-consuming, not requiring the preparation of PRP from the citrated whole blood. Platelet aggregometry involves a series of tests performed on whole blood or platelet-rich plasma, using several agonists (platelet activators). The agonist is added to

the suspension and a dynamic measure of platelet clumping is recorded. Platelet Aggregometry

The most common aggregation agonists are:

- **Arachidonic acid**: used to assess the viability of the thromboxane pathway.
- **Thrombin**: reacts with several membrane sites to induce full aggregation and secretion of organelle contents independent of the prostaglandin or ADP pathways.
- **ADP**: binds to a specific platelet membrane receptor and causes platelet activation and release of dense granule stored ADP. Shows biphasic aggregation.
- **Epinephrine**: binds to specific receptor and causes ADP secretion, but does not cause aggregation in storage pool disorder or release defects.
- **Collagen**: Shows no primary wave of aggregation and depends on intact membrane receptors, membrane phospholipase pathway integrity and normal cyclooxygenase and thromboxane pathway function.
- **Ristocetin**: requires VWF and intact surface membrane including a functional vWF receptor site (GPIb).

1.1.2.2 PFA-100

The platelet function analyzer-100 (PFA-100 Siemens Healthcare Diagonstics Inc, USA) is a primary hemostasis test, particularly an adhesion assay. It is system for analyzing platelet function in which citrated whole blood is aspirated at high shear rates through disposable cartridges containing an aperture within a membrane coated with either collagen and epinephrine (CEPI) or collagen and ADP (CADP) [22]. These agonists

induce platelet adhesion, activation and aggregation leading to rapid occlusion of the aperture and cessation of blood flow termed the closure time (CT). An advantage of the PFA-100 is that only small volumes of citrated venous blood (800µL) are needed and so the test is useful for investigating platelet function in children. However, many different variables (citrate concentration, collection time, platelet count, VWF levels) can negatively affect results.

1.1.2.3 VerifyNow

The VerifyNow™ (Accumetrics, USA) is used to evaluate primary hemostasis. It is turbidimetric based optical detection system which measures platelet induced aggregation as an increase in light transmittance [23]. The system consists of an instrument, a disposable assay device and controls. The assay device contains reagents based on microbead agglutination technology. The assay device contains a lyophilized preparation of human fibrinogen-coated beads, platelet agonist, preservative and buffer. The patient sample is 3.2% citrated whole blood, which is automatically dispensed from the blood collection tube into the assay device by the instrument, with no blood handling required by the user.

1.1.2.4 TEG Platelet Mapping

The whole blood Thrombelastograph (TEG®) Platelet Mapping™ assay is a global hemostasis test, meaning it measures both primary and secondary hemostasis. The PlateletMapping™ assay was introduced to monitor anti-platelet therapy by TEG [24]. A

native blood sample activated by kaolin is compared with heparinised samples where the fibrin network is formed by adding reptilase and FXIIIa and the platelets are activated by ADP or arachidonic acid.

1.1.3 Novel Whole Blood Thrombus Monitoring Technology

This section will describe that different tests used to measure whole blood thrombus formation. These technologies have not yet been tested in pediatric ECLS.

In general, there are only major limitation associated with current whole blood thrombus technologies is that these tests do not incorporate the effects of the endothelium in global hemostatic assessment.

1.1.3.1 Total Thrombus-formation Analysis System (T-TAS)

T-TAS (Fujimori Kogyo) is a microfluidic perfusion chamber system that measures global hemostasis. It is considered an adhesion assay. T-TAS (Total Thrombus formation Analysis System) is an automated microchip flow chamber system for the quantitative analysis of the thrombus formation process under blood flow conditions [25]. T-TAS reproduces the in vivo thrombus formation process in an *ex vivo* system that uses the same substances that stimulate thrombus formation under physiological conditions. Therefore, T-TAS enables the *ex vivo* evaluation of overall hemostatic ability that more closely reflects the in vivo condition than other tests. Two types of T-TAS systems have been developed: T-TAS 01 for clinical use, equipped with two measuring channels and animated operation guide for efficient measurement, and T-TAS PLUS for research use,

having additional functions of user-selectable flow rates and real time observation of thrombus formation with a CCD camera.

The T-TAS system accepts two different types of microfluidic chips. The AR-100 chip is coated with collagen and tissue factor, and can measure global hemostasis. On the other hand, the PL-100 is coated with just collagen and is used to assess platelet function [26]. For both chips thrombus formation is measured using a pressure sensor. As the microchannel becomes occluded the pressure increases. However, if the blood is less thrombogenic which can be due to a variety of different reasons then the pressure will not rise as much. The T-TAS system is currently being evaluated for different clinical indications such as predicting bleeding risk during surgery and monitoring both anticoagulant (DOACS) and platelet transfusion therapies [27]. In terms of research use, the T-TAS has mainly been used to evaluate the efficacy of novel anticoagulants (DOACs, NOACs, DTIs) in both venous and arterial shear rates [27].

The T-TAS system has yet to be tested in pediatric patients on extracorporeal life support. However, since the microchips use less than 500µL of blood it does meet the low blood sample requirements for pediatric critical care blood testing. A potential disadvantage of this system may be related to the design of the microchip which is a straight microchannel. As a result, perfused blood is subjected to a continuous shear rate through the length the experiment. However, *in-vivo* blood is exposed to varying shear rates which arise from different vascular architectures. Therefore, perhaps this system can be improved if its microfluidic design was modified to make it more physiologically-relevant.

1.1.3.2 Biomimetic Whole Blood Global Hemostasis Test

The Shear-Activated Whole Blood microfluidic system measures global hemostasis. It is considered an adhesion assay [11]. The microchip part of this system was designed to mimic of bed of stenosed arterioles. This architecture exposes flowing blood to pathological fluid shear rates and gradients which act to mechanically drive the global hemostatic process. Furthermore, the microchip is coated with collagen a prothrombotic protein that promotes the activation of platelets and initiates the intrinsic pathway of the coagulation cascade. A pressure sensor is used to measure microchannel occlusion and detect blood abnormalities.

A novel aspect of this system is that it used a phenomenological mathematical model to quantify the time at which the microchannels were occluded with thrombus. This model was based on the observation that fibrin formation follows a sigmoidal trend. Then a two-parameter exponential growth curve (reciprocal of sigmoid) was used to fit this curve. A clotting time was derived which was determined to be the time the pressure rises to 2.86 times the initial pressure. The clotting time was used to demonstrate that the biomimetic microdevice was sensitive to heparin, shear rates, extracellular matrices, anti-platelet medications, dysfunctional platelets. Importantly, this clotting time was used to monitor LPS induced coagulopathy and heparin therapy in pigs *ex vivo*.

Based on these preliminary results, the biomimetic system described above shows promise for monitoring global hemostasis in pediatric extracorporeal life support patients. However, despite being biomimetic, this test requires more than 1mL of blood and would

need to be further optimized to reduce blood volume consumption which is a limiting resource in this patient population.

2. MICROENGINEERED TORTUOSITY-ACTIVATED DEVICE FOR MEASURING THROMBUS, COAGULATION AND PLATELET FUNCTION IN PEDIATRIC PATIENTS ON EXTRACORPOREAL LIFE SUPPORT

2.1 Design and Computational Analysis of a Tortuous Microchannel

We initiated our project by investigating the design features of a single tortuous microchannel. As stated, tortuous vessels have been shown to induce fluid dynamical disturbances and shear gradients that make them hotspots for forming thrombi *in vivo* [12]. Also, some prior studies have shown increased thrombosis due to tortuosity *in vitro* [13].

2.1.1 Tortuous Channel Design

The tortuous channels were designed as simple sinusoidal curves governed by the equation $y = \sin \alpha x$, where α is the frequency of the sinusoid and x is horizontal Cartesian coordinate. The arc length of these tortuous channels was then calculated according to the following relation:

$$f(x) = \sqrt{1 + \alpha^2 \left(\cos(\alpha x)\right)^2} \tag{1}$$

$$TI = \frac{\alpha}{\pi} \int_0^{\pi/\alpha} f(x)$$

The tortuosity index was calculated as the ratio of the arc length of the curve to the end-to-end distance of the curve. We set the primary dimensions (width, height and length) of the microchannel to be 200 um, 75 um and 2 cm respectively, so that it mimics the size a

typical arteriole of an equivalent diameter ~100 um, but is also easy to fabricate, imaged, perfusable with blood, and fits on a standard glass slide. Next, using Solidworks software, we designed microchannels of varying tortuosity indices (Fig 2-1), but kept the width, height, length and amplitude constant, as given. We found that within the given parameter space, we could design microchannels with a TI ranging from unity (straight channel) to a maximum of 3.4 (30^0 arc angle), beyond which the channels cannot bend.

2.1.2 Computational Fluid Analysis

Next, finite element-based software, Ansys Fluent (Ansys INC, Canonsburg, PA) was used to simulate blood flow inside the tortuous microchannels. The Solidworks line drawing of the microchannels were exported in .stl format to Ansys. Blood was assumed to be a two-dimensional incompressible fluid, homogenous and non-Newtonian. A high-density finite element mesh was constructed for precise calculations. The Navier-Stokes equation of fluid dynamics was solved by assigning a finite velocity as the inlet boundary condition and constant atmospheric pressure (P=0) at the outlet boundary. To describe the stress-strain relationship and blood viscosity, a generalized power-law constitutive equation for non-Newtonian fluids was applied and parameters were chosen based on published values [28]. Ansys was able to calculate and export the values of wall shear rates along the selected boundary edges during post processing.

2.2 Results and Discussion

2.2.1 Tortuous Microchannels

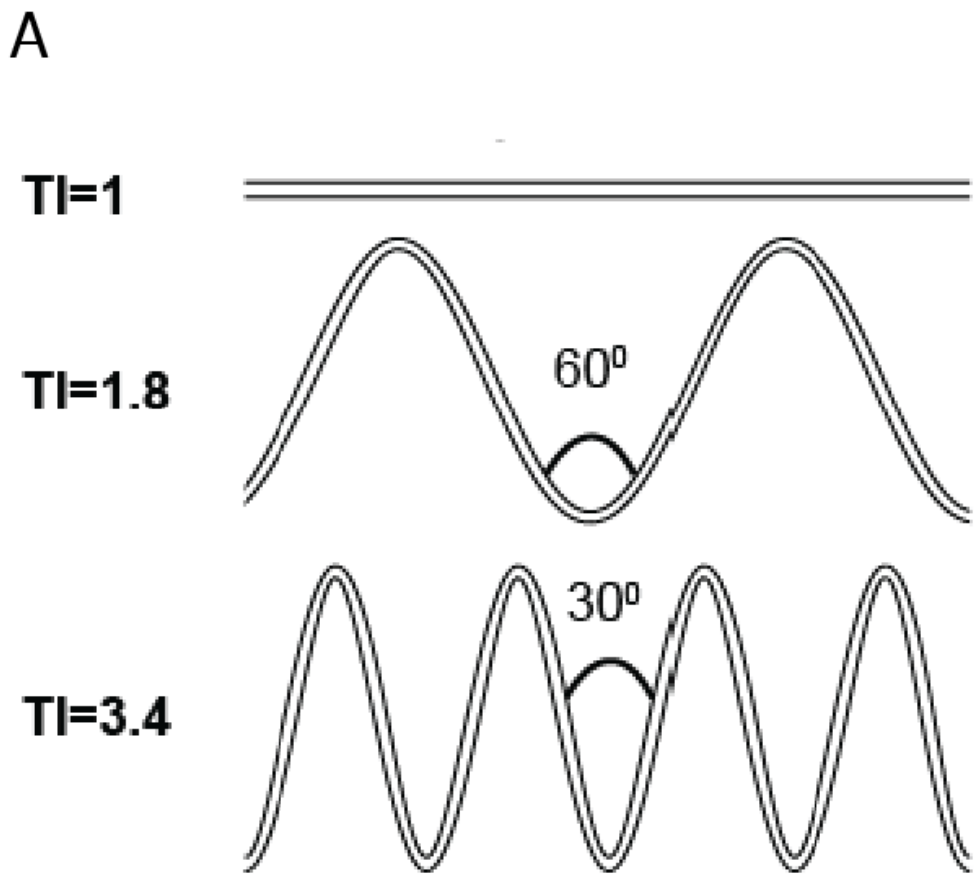

Figure 2-1. Illustration of various tortuous curves (TI 1.0, 1.8, 3.4).

2.2.2 Computational Fluid Dynamic Profile in Tortuous Microchannels

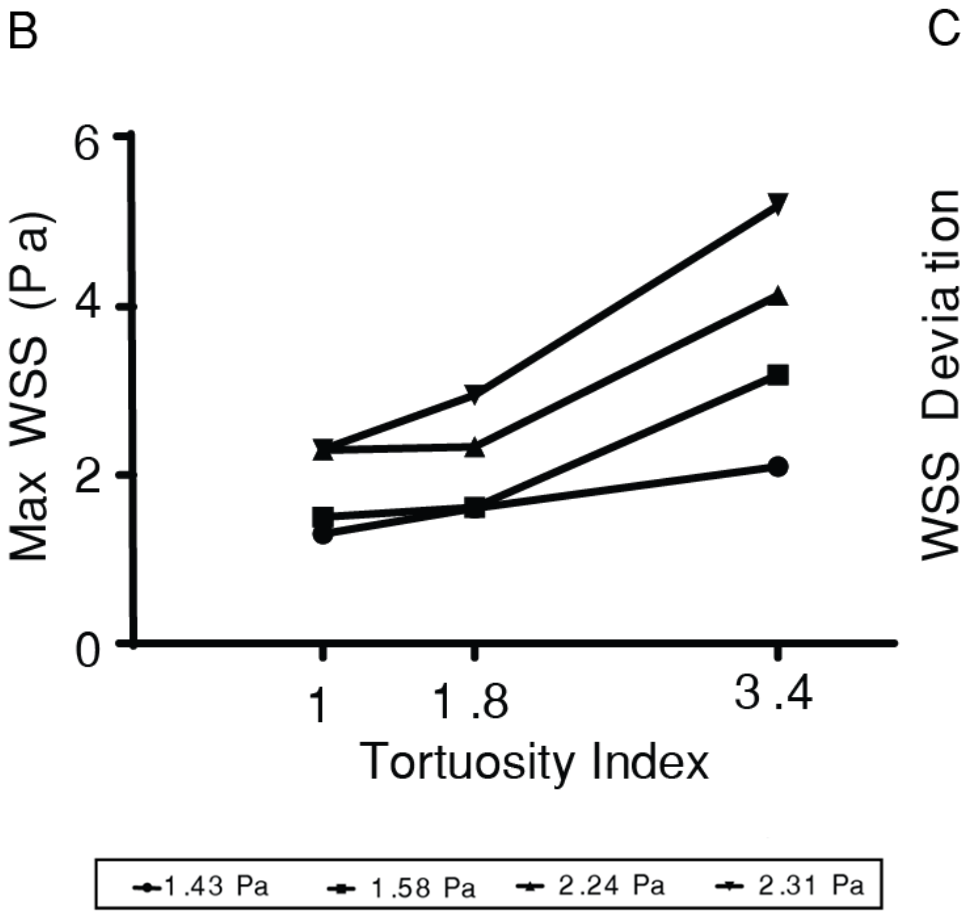

Figure 2-2. Graph showing the maximum wall shear stress as a function of tortuosity and imposed dynamic pressure.

These analyses showed that the maximum wall shear stress increase with increasing tortuosity and imposed pressure drop across the channel (Fig 2-2).

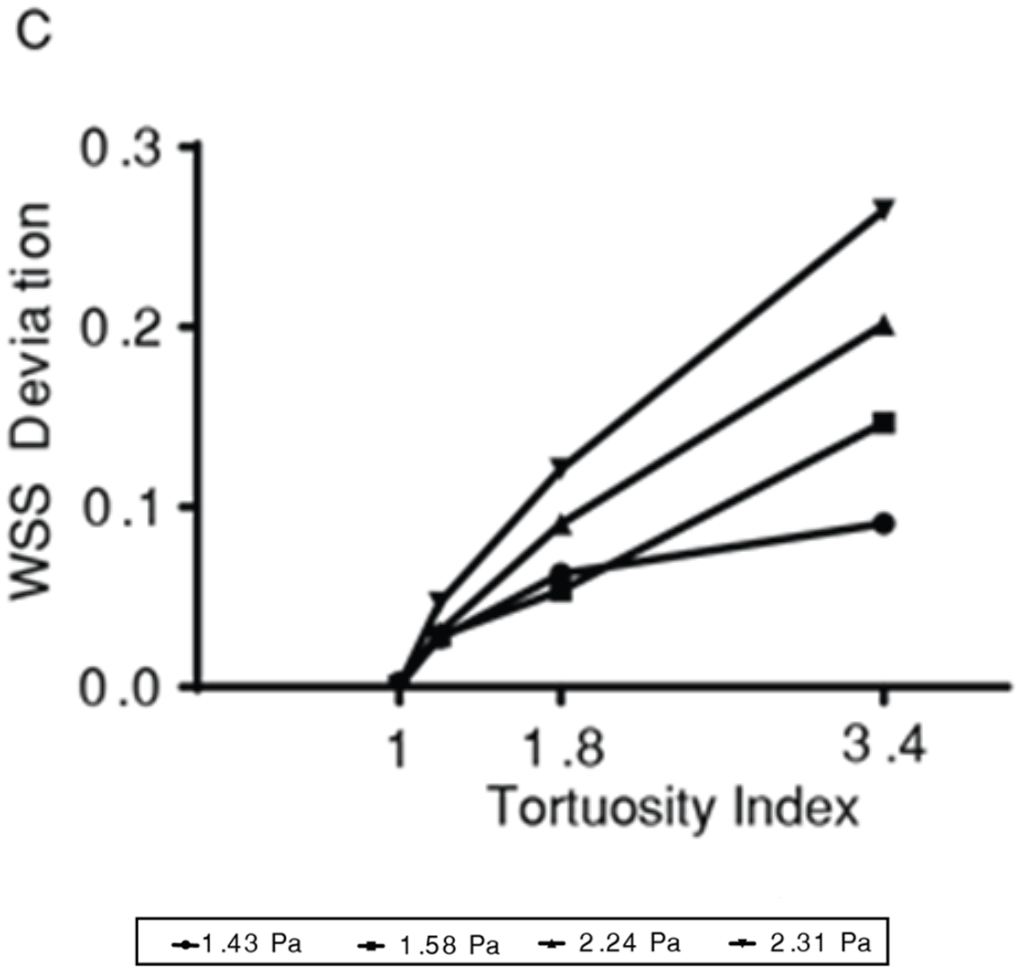

Figure 2-3. Graph showing wall shear stress gradients (deviation from mean) as a function of tortuosity and imposed dynamic pressure.

Importantly, our analysis showed that tortuous vessels also led to fluid shear gradients (acceleration and deceleration of flow) across the microchannel that also increased with tortuosity (Fig 2-3). These predictions suggested that upon blood clot formation in the device, the occlusion may be fastest and use minimum blood volume if the channels are most tortuous (TI 3.4) and blood is perfused through the device at a high flow rate. Thus, based on this analysis, we set a TI=3.4 for a single microchannel of our device.

2.3 Design and Computational Analysis of a Stenosed - Tortuous Microdevice

Our objective here was to integrate the shear gradients induced by stenosis to tortuosity-driven gradients in the microdevice, so that blood clots may form rapidly and require low blood volume for testing in pediatric patients on extracorporeal membrane oxygenation (ECMO).

2.3.1 Biomimetic Device Design

We designed a microfluidic device containing microchannels that mimic stenosed tortuous arterioles to create sudden fluid acceleration (pre-tortuous), followed by a region of non-uniform shear (tortuous region), and then by a region with a sudden deceleration (post-tortuous), when whole blood is perfused through the device (Fig 2-4). This was achieved by allowing the blood to first enter into a large reservoir (4.7 mm wide, 75μm high) and then splitting the flow into four smaller parallel tortuous channels (TI = 3.4) (200μm wide, 75μm high); followed by convergence of the flow into an outlet similar to the inlet. Each device contains multiple single microchannel sections that were optimized to create maximum tortuosity (alternating 30^0 bends, corresponding to TI = 3.4), to expose flowing whole blood to varying shear rates, thus promoting rapid clot formation and occlusion. Furthermore, the 4-channel design was chosen to better mimic clotting within a natural blood vessel network than using one very long channel, which would more closely resemble a single occluded channel. Also, this design is analogous to clotting within multiple vessels of a vascular network that occurs in living patients with coagulopathies

in vivo where clots may form, deform, translocate and detach locally, but the pressure still increases in the vascular bed due to the systemic response to thrombosis. In addition, the total width and length of the device were designed to fit on a standard glass microscope slide to enable simultaneous real-time optical microscopic imaging using a low magnification objective, while ensuring near homogenous flow in all parallel tortuous channels.

2.3.2 Computational Fluid Dynamic Analysis

Finite element-based software, Ansys Fluent (Ansys INC, Canonsburg, PA) was used to simulate blood flow inside the microdevice. The Solidworks line drawing of the microdevice were exported in .stl format to Ansys. Blood was assumed to be a two-dimensional incompressible fluid, homogenous and non-Newtonian. A high-density finite element mesh was constructed for precise calculations. The Navier-Stokes equation of fluid dynamics was solved by assigning a finite velocity as the inlet boundary condition and constant atmospheric pressure (P=0) at the outlet boundary. To describe the stress-strain relationship and blood viscosity, a generalized power-law constitutive equation for non-Newtonian fluids was applied and parameters were chosen based on published values [28]. Ansys was able to calculate and export the values of wall shear rates along the selected boundary edges during post processing.

2.4 Results and Discussion

2.4.1 Stenosed -Tortuous Biomimetic Microfluidic Device

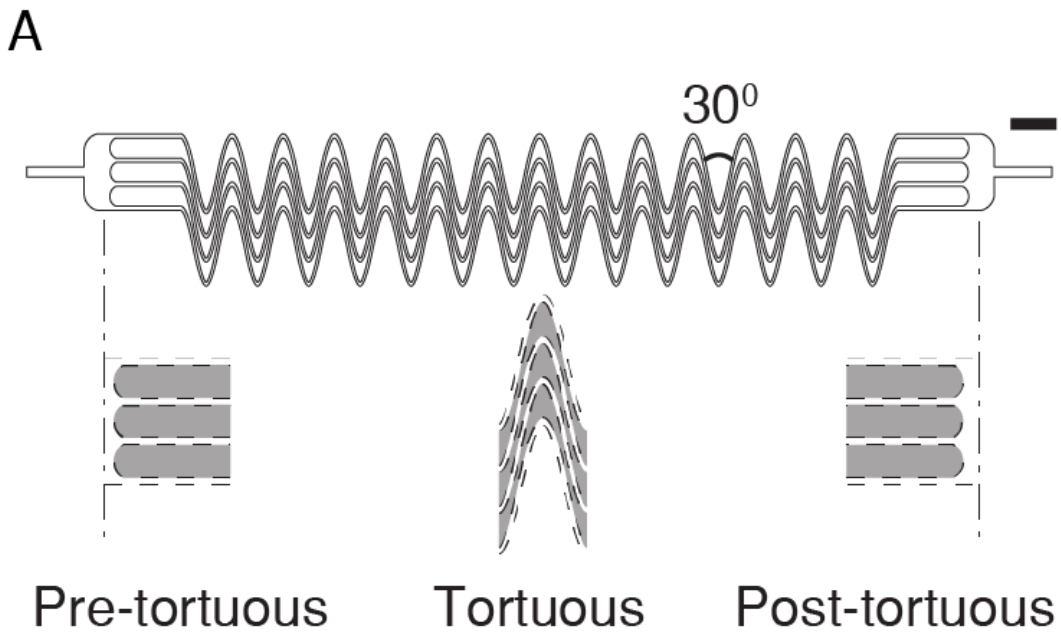

Figure 2-4. Diagram of microdevice with line drawings below showing the design of the accelerating (pre-tortuous), uniform region (tortuous) and decelerating (post-tortuous) regions of the microchannels. The central tortuous region contains 4 parallel tortuous lanes that are 200μm wide by 75μm high that repeatedly turn 30^0 frequently in each channel (scale bar 1mm).

2.4.2 Computational Fluid Analysis of Biomimetic Design

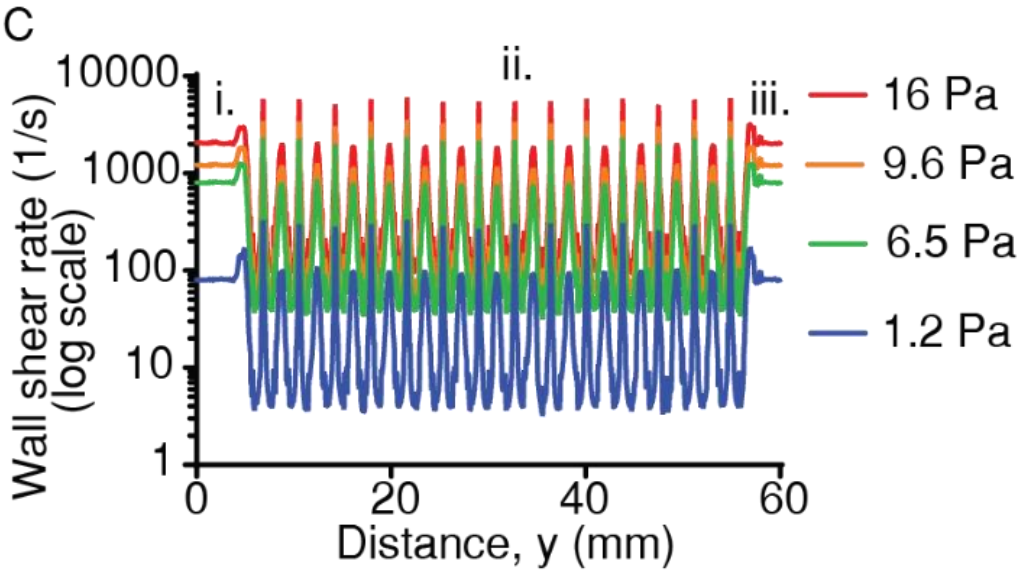

Figure 2-5. Graph showing results of computational modeling of blood flow through the device. The wall shear rate across the length of the entire device (i. pre-tortuous, ii. tortuous, iii. post-tortuous; from left to right) is shown for various imposed dynamic pressures (1.20- 16.0 Pa).

Computational analysis of non-Newtonian blood flowing through the device confirmed that for a given imposed pressure inlet boundary condition, the wall shear rate rapidly changes at the pre-tortuous and post-tortuous regions as shown in our previous study [11]. But by introducing tortuosity, we saw that shear also fluctuates significantly in the tortuous region, creating a pathological and prothrombotic fluid mechanical environment within the device (Fig 2-5). Moreover, we saw that the absolute wall shear rate as well as its gradients increased with increasing imposed pressure, indicating that blood clot formation may be enhanced at higher flow rates. Thus, this design was found to have three distinct

shear gradient zones: pre-tortuous, tortuous and post-tortuous which together accelerate blood clotting.

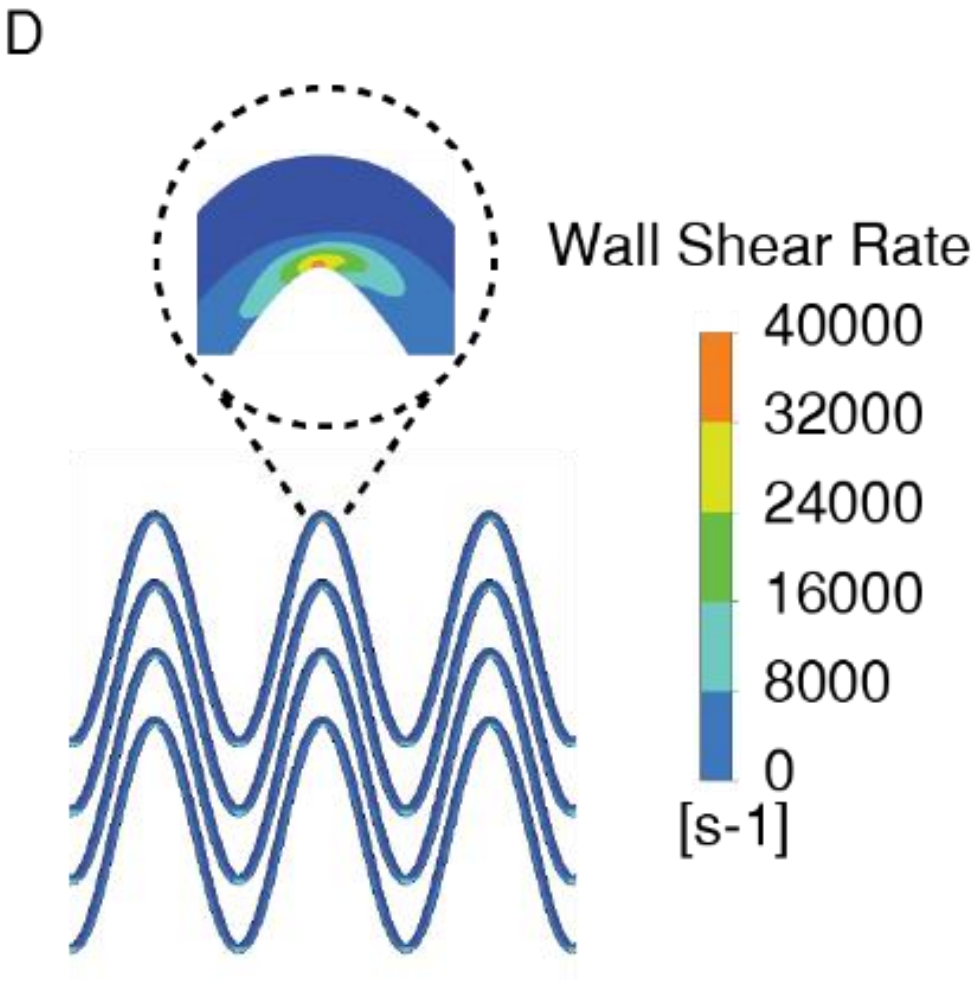

Figure 2-6. Representative wall shear rate (1/s) profile in the tortuous region.

Moreover, we show that the wall shear rate (γ) repeatedly spiked at the inner curve and then dipped at outer curves of the tortuous channels, confirming the presence of many clot inducing shear gradients in the tortuous region (Fig 2-6). In practice, we operated the device at a flow rate of 70 µl/min, leading to a pre-tortuous wall shear gradient of 935

1/s/mm, which corresponds to a mean wall shear rate of 1200 1/s (20-25 dynes/cm^2) in the straight region following the pre-tortuous reservoir which is typical arteriolar flow. This flow rate was chosen because flow rates outside this range were undesirable as they would require much larger volumes of human donor blood.

2.5 Microengineering

There are numerous methods to fabricate microfluidic devices. The methods we utilized include photolithography of a master mold followed by soft lithography of a polymer on the mold to fabricate microfluidic devices [29].

2.5.1 Process

As mentioned above the microdevice was designed using Solidworks. Then, the microdevice design was printed on a transparent mylar sheet using a high resolution (400,000dpi) printing system. This film serves as a mask for the photolithographic process. During this process the mask is sandwiched against a Si (100) wafer (University Wafer Corp.) coated with negative photoresist, SU8 2075 (MicroChem. Corp.). Next, the wafer-resist-mask sandwich is exposed to ultraviolet (UV) light in the photolithography aligner. The UV light passes through the mask onto resist which causes a cross linking of the resist polymers. We then remove the mask and place the wafer with resist into the developer which causes the removal of the unexposed resist. The part of resist left forms a 3D template of master. The master is a positive relief of the final structure. To fabricate

the microfluidic structure, Slygard 184 polydimethylsiloxane (PDMS) prepolymer is poured over the top of a silanized master. The polymer is subsequently cured and removed from the master. PDMS is used because it is transparent and inexpensive.

2.5.2 Materials

Polydimethylsiloxane (PDMS) is a widely used material used for soft lithography. One of the main characteristics of PDMS is that it is hydrophobic in its native state. The hydrophobicity of PDMS is due to the presence of methyl groups in its structure[16]. However, the methyl groups can be converted to hydroxyl groups using an O_2 plasma treatment that makes the PDMS surface temporarily hydrophilic [30]. Oxygen plasma treatment also results in an irreversible bond with a glass substrate.

2.5.3 Master Fabrication

As explained in the process section, the PDMS replica molding is done over a silicon master. The following sections describe the fabrication process for making a master.

2.5.3.1 Mask Design

We design the photomask on Solidworks 2018 (Dassault Systemes, Waltham, MA). We aimed to fit as many designs as possible within the dimensions of the actual wafer on which patterning will occur. The wafer size typically used to 4” circular diameter. The basic design rules for designing are as follows:

1. The design should be made using polylines and the pattern should be closed, i.e. all lines should be perfectly joined.
2. Masks for negative photoresist (SU8) must be printed with black background and transparent patterns.

For feature sizes larger than 20µm, the masks should be printed on a mylar transparency sheet.

2.5.3.2 Photoresist Patterning

We used a 4" circular diameter silicon (Si) wafer as a substrate. If the substrate was not clean, we performed the 3-step cleaning process. The 3-step cleaning process is described as follows:

1. Rinse with Iso-propyl alcohol (IPA)
2. Rinse with Methanol
3. Rinse with Acetone

Following the cleaning process, we put the wafer in 120°C oven for 1 hour to dehydrate it.

Next, we created a thin SU-8 2075 photoresist layer on a planar substrate by spin-coating. This was done by applying an initial ramping stage from stop to 500 rpm at an acceleration of 100 rpm per second to spread the photoresist and cover the entire wafer. We then accelerated the spin speed at a rate of 100 rpm per second to the final speed of 3000 rpm and held for a total of 30 s. The thickness of the photoresist layer is determined by the final rotational speed during spin-coating and the viscosity of the photoresist.

Approximate correlations between spin speed and the resulting photoresist thickness are provided by the supplier [31]

2.5.3.3 Soft Baking

Following the spin coating step, we soft bake the wafer. The soft bake process is the most critical step in SU-8 processing because it determines the quality of the photolithography. A uniform and optimal baking temperature and time are required. Short bake time or lower temperature can cause the resist to peel off during the development stage whereas a long bake or higher temperatures can result in thermal stresses on the resist that can result in deformed patterns after development. With the baking step, the solvent in SU-8 are evaporated and the photoresist is condensed. Soft bake temperatures and time are provided by the supplier. Initially, 2 minute back at 65°C ramps the temperature of the substrate and photoresist, allowing the solvent to evaporate out of the film at a steady rate. This improves the coating fidelity and adhesion to the substrate, while also reducing the edge bead. A subsequent longer bake of 4 minutes at 95 °C continues the evaporation and condensation process. We used an aluminum top hot plate because it provides a more uniform heating of the wafer.

2.5.3.4 Exposure

We expose the substrate with the SUSS MA6 exposure tool in AggieFab cleanroom at Texas A&M. The mylar mask is pasted on a plain 5” by 5” piece of glass to provide mechanical support so that the MA6 could hold the mask using air suction. The exposure of SU-8 results in production of an acid that initiates the crosslinking of photoresist. The UV exposure of photoresist creates a “front” of exposed resist, which grows out from the addressed surface with increasing exposure time. Insufficient exposure doses are unable to adequately initiate polymerization throughout the thickness of the photoresist and transferred patterns do not resist slight dissolution during the development stage. Detachment from the substrate surface can occur in cases of extreme underexposure. An upper limit to the exposure dose also exists. Over-exposing results in the creation of “shadows” or finite areas of partially exposed photoresist around the desired features due to a combination of Fresnel diffraction at the edge of opaque sections, refraction at the air-photoresist interface, and reflection from the base substrate.

2.5.3.5 Post Exposure Bake

Following the exposure step, we baked the substrate for 8 min at 95°C to accelerate the crosslinking reaction. Inadequate post exposure bake times will result in poorly cross-linked resist structures, which can cause the deterioration or failure of the transferred design during developing. Care must be taken to minimize stresses that are induced during the post- exposure bake. In extreme cases, stresses in the film can cause photoresist cracking and bowing of flexible substrates.

2.5.3.6 Development

We develop the master using the standard SU-8 developer (1-methyl-2-propyl acetate). The time required to completely remove unexposed photoresist is dependent on the photoresist thickness, level of agitation or vibration, minimum feature size of the exposed pattern, and history of (previous use) of the developer solution. While it is possible to determine an optimal development time for a given photoresist structure, this Would be unique for the combination of the aforementioned parameters and as such is of little benefit to the rapid prototyping process. Developing can be visually inspected until the process is complete. The removed resist will restore the shine of the wafer beneath it. Typically, the time is 2-4 minutes. A subsequent rinse with isopropyl alcohol serves to both arrest the development process by removing developer and indicate if development is complete. Water should never be used for rinsing after development. Unexposed photoresist remaining on the surface turns into a white, flaky material during the isopropyl rinse.

2.6 Results and Discussion

2.6.1 SU-8 Wafer Characterization

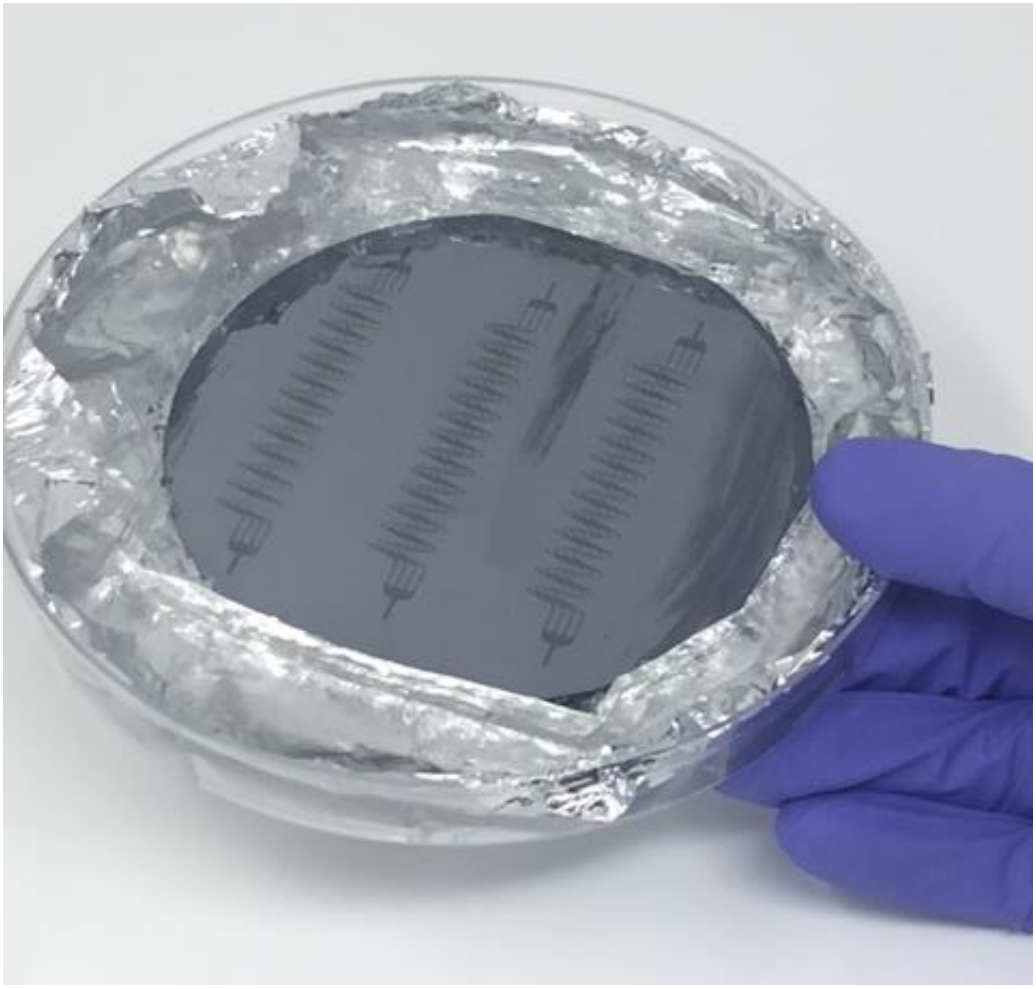

Figure 2-7. Picture of SU-8 master mold

A silicon wafer with the negative photoresist positive of the tortuosity-activated design (Fig 2-7).

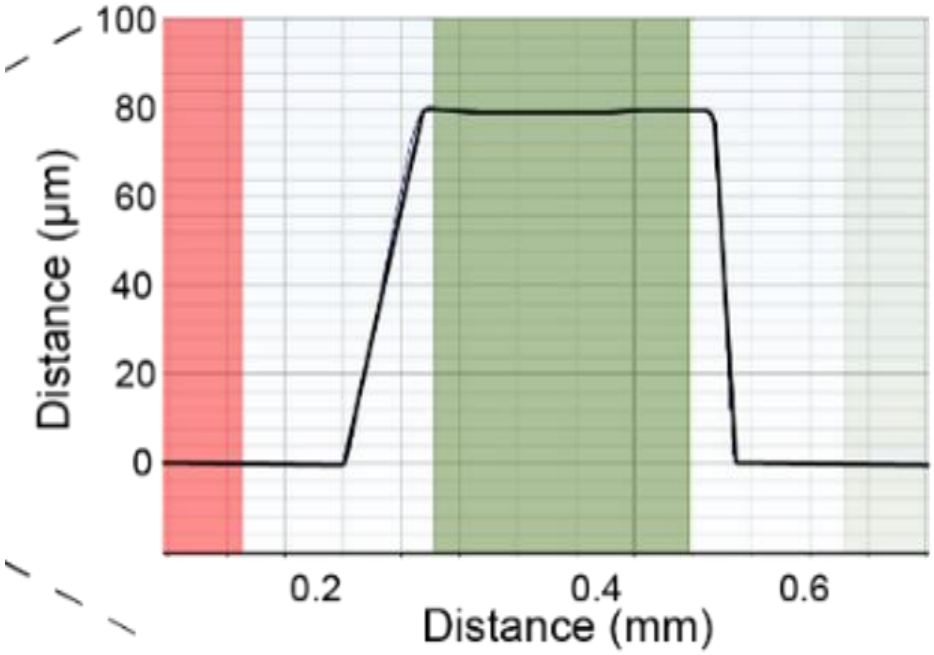

Figure 2-8. Profilometer measurement of SU-8 microchannel

The profilometer machine confirmed that the microchannel dimensions were 200µm wide by 75µm high, having a hydraulic diameter similar to a typical arteriole (Fig 2-8).

2.7 Microfluidic Device Fabrication

The soft lithography of PDMS can be done in a class-1000 or class 10,000 room depending upon the criticality of the process. The process is described in Figure 2-9.

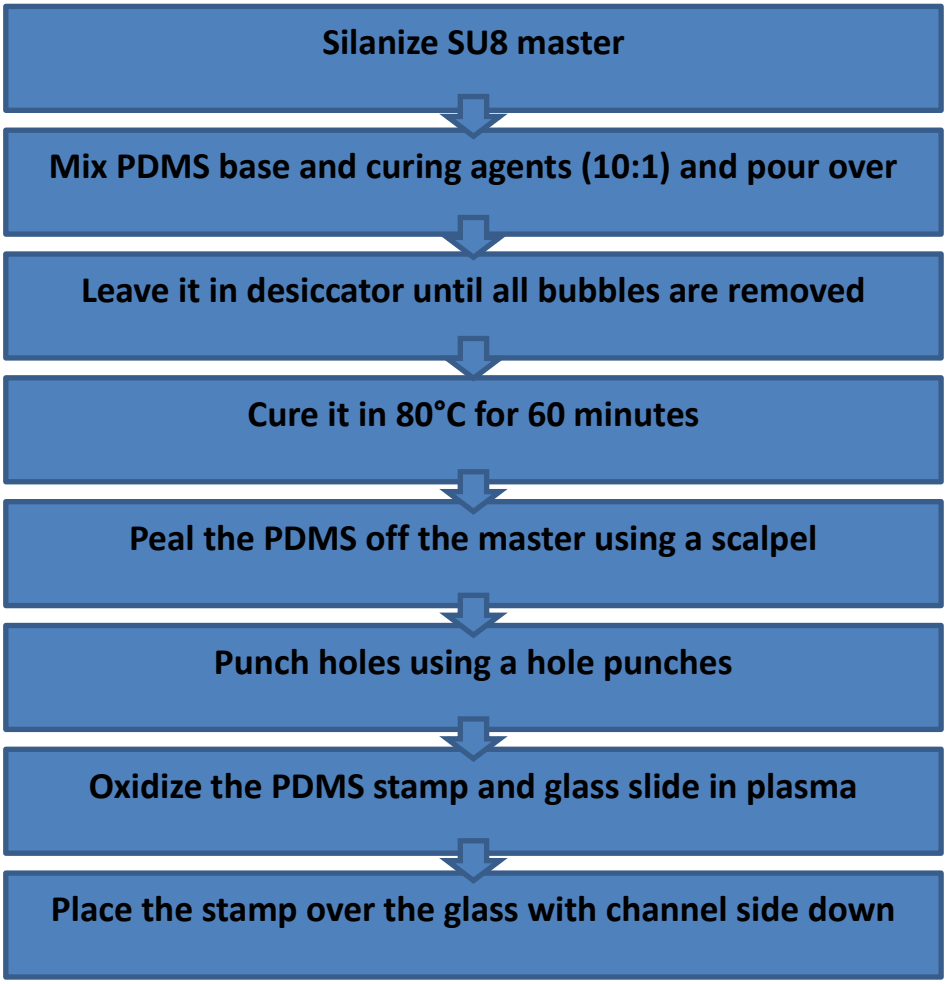

Figure 2-9. Flowchart of PDMS Soft Lithography Process

2.7.1 Silanization of Master

Silanization of SU-8 master is important because it prevents the PDMS from sticking to the wafer. Improper silanization can destroy the master completely. The silanization can be done using tri-chloro-methyl-silane (TCMS). It is a very hazardous chemical and proper safety precautions should be taken to handle TCMS as given in its material safety data sheet (MSDS). Vapor deposition is a well-established method to deposit silane over a wafer. Vapor deposition is a self-limiting reaction. We place the wafer on top of pipette tips that are fitted into a ceramic covering with holes. Below the ceramic we place a plastic weighing disk that contains 100 µl of TCMS. The wafer and silane are then desiccated for 8 hours. After silanizing PDMS can be poured over the master.

2.7.2 Casting PDMS on Master

We used Slygard 184 PDMS to make our devices. PDMS comes in 2 parts, base agent and curing agent. The standard mixing ratio of the two is 10:1 by weight respectively. Using less base agent results in more stiff PDMS and can result in cracking. Using base agent results in softer PDMS. We measure PDMS by weight using a standard electronic balance (Fisher Scientific, Waltham, MA). We mixed the 2 parts using a Thinky Mixer which both mixes and degasses the PDMS (Thinky USA). After mixing we placed the PDMS in a desiccator until all bubbles were removed. Before pouring the PDMS, care is taken to remove any contaminants from the silanized wafer using a Nitrogen gun. Next, the PDMS is cured in an 80°C convection oven for 1 hour.

2.7.3 Removing, Hole Punching, and Bonding

We removed the PDMS from the master using a scalpel. After the PDMS has been removed, we punch holes at the inlet and outlets. The holes are punched to an OD of 1.5 mm (Ted Pella). Before oxygen plasma treatment and bonding we clean the PDMS with scotch tape to remove particulate matter. Next, the glass slide and PDMS stamp are treated with oxygen plasma (100 W, 30 s). After the plasma treatment the PDMS is placed over the slide immediately, resulting in an irreversible bond (Fig 2-10).

2.8 Results and Discussion

2.8.1 Stenosed-Tortuous Biomimetic Medical Device

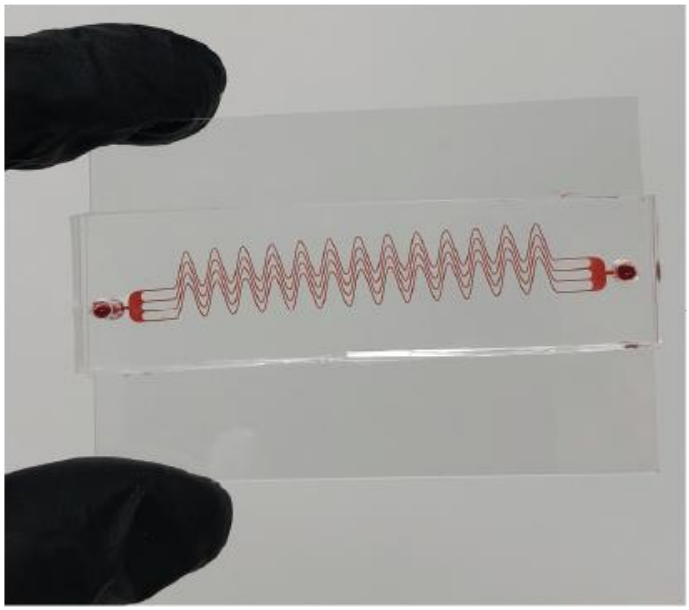

Figure 2-10. Photograph of the microdevice on top of a standard glass slide with whole blood in microchannels (75mm x 50mm)

2.9 In-Vitro Evaluation of Microdevice Sensitivity to Anticoagulants via Imaging

Precise and personalized anticoagulant dose monitoring is critical in patients on extracorporeal life support systems (ECLS) to ensure therapeutic anticoagulation to avoid life threatening bleeding episodes and also to prevent clotting in the blood transport lines and pumps of these devices *in vivo* [1-3]. This requirement is particularly more stringent in pediatric patients. To explore the potential utility of using this microfluidic device as an anticoagulant dose monitor, we tested its sensitivity to clinically relevant doses of unfractionated heparin (UFH) the most commonly administered anticoagulant in pediatric critical care settings. Furthermore, we explored if our device can also detect differences in doses of bivalirudin, since bivalirudin is being increasingly prescribed as an alternative to heparin in pediatric critical care clinics [32-34]. But while the use of bivalirudin has shown promising results in a few clinical studies, routine coagulation monitors cannot help its dose and timing accurately and reliable [35-37]. As a result, it is challenging to prescribe bivalirudin as an alternative anticoagulant

2.9.1 Experimental Approach

2.9.1.1 Microdevice Fabrication

The stenosed-tortuous microfluidic PDMS device was fabricated using the soft lithography process as described previously in section 2.7.

2.9.1.2 Collagen Coating Process

This section will describe the process of coating the stenosed-tortuous microfluidic device with collagen. Collagen is an extracellular matrix protein that surrounds the endothelium of a blood vessel. When the endothelium is injured, collagen in the sub-endothelium is exposed to the blood where it acts as a platelet agonist, aiding in the adhesion, activation and aggregation of platelets [38].

First, the PDMS device is placed in the plasma machine and treated with oxygen plasma (45 s, 100W) to oxidize the PDMS surface. Oxidizing the PDMS promotes hydroxyl groups which react with chemical groups on the collagen to allow for strong collagen adhesion. Immediately, after plasma treatment, 100µg/mL of collagen type 1 (rat/horse/human) diluted in PBS (-/-) is pushed via 1mL slip tip syringe through a 1.5 mm OD barbered connector in the inlet port of the device. Next, the collagen coated devices are placed in a petri dish and submerged in PBS (-/-) with 1mL slip tip plugs connected to the slip tip side of the 1.5 mm OD barbed connector in each port to prevent leaking and incubated in 5% CO_2 for 1 hour.

2.9.1.3 Assembly of Microfluidic Device for Fluorescent Imaging

This section will describe how to assemble the stenosed-tortuous microdevice with a reservoir and tubing for use in whole blood perfusion experiments.

To make a reservoir to hold whole blood:

1. Acquire a 5mL slip tip syringe (Bection Dickson)
2. Remove plunger
3. Cut syringe at 3mL mark with PVC pipe cutters

After 1 h of incubation, remove the 1mL slip tip syringe from 1.5 mm barbed connectors while leaving the barbed connector attached to inlet and outlet ports. Next, connect the reservoir to the slip tip side of the barb connector. Next, acquire a 10mL male luer lock syringe and draw up 5 mL PBS (-/-) and connect it to the female luer side of tubing. Push the PBS (-/-) through the tubing until it reaches the slip tip end then connect it the slip tip end of the barbed connector that is attached the outlet port of the microfluidic device. Gently push PBS (-\-) though the microfluidic device and check to see if PBS (-
-) is filling up the reservoir. If you push too hard on the syringe this may cause collagen that is not strongly coated to the PDMS glass slide to delaminate, thus resulting in less platelet adhesion when performing downstream whole blood experiments.

2.9.1.4 Monitoring Effect of Anticoagulants on Fibrin Formation via Fluorescent Microscopy

Healthy blood samples were collected after informed, written consent as per ethical guidelines of Institutional Review Board of Texas A&M University. Healthy donor blood

was collected from non-smoking volunteers in a 3.2% 2.7mL sodium citrate vacutainers (BD). Coagulation experiments were initiated within 30 minutes after the blood draw.

The process to acquire fluorescent images of thrombus formation is described here. First, set the flow rate to 70 µL/min (corresponds to 1,200 1/s which is a typical arterial shear rate) on the Harvard Apparatus syringe pump. Next, load 1 mL of fresh blood sample into the microdevice reservoir and subsequently add 15 ug/mL of fibrinogen (Alexa Fluor 647, Invitrogen) and clinically relevant doses of either heparin (IU/mL) or bivalirudin (µg/mL) to the blood sample. Mix the solution well with a 1mL pipette. Next, take the microdevice to the fluorescent microscope (Zeiss Observer Z1) and load it onto the microscope, then load the 10mL syringe onto the syringe pump. Next, open the ZEN software and find the correct settings for time-lapse imaging (x 10, numerical aperture 0.35; Zeiss Observer Z1). Next, because the whole blood is anticoagulated with citrate, the coagulation activity of these samples were restored by adding 100uL/mL of 100mM calcium chloride/75mM magnesium chloride solution. Immediately after the recalcification solution is added to the blood, start pulling the blood through the device and acquiring fluorescent images of fibrin for 15 minutes. After perfusion, acquire wide-field fluorescent images of the entire device to observe fibrin volume in different regions of the device.

2.9.1.5 Quantification of Fibrin Area Coverage

Here we will describe the process of quantifying area coverage from fluorescent images. First, in the zen software convert the czi. file of the image to a OME-TIFF. If needed, you can also convert an area of interest. Next, import the OME-TIFF images into the Matlab script in appendix A.

The MATLAB script does the following: It reads all of the pixels in the image, and their corresponding intensities, and then applies a threshold to the pixel intensities. If the pixel intensity is below the threshold then it will be computed as a 0, whereas a pixel intensity that is above the threshold will be a 1. Therefore, areas in the image with fibrin rich thrombi will be read as 1's and areas with low amounts of fibrin will 0's. Next, all the 1's are summed and divided by the total number of pixels in the image, resulting in fibrin area coverage.

2.9.1.6 Statistical Analysis

In vitro assay sample size was predetermined with three separate healthy donors to account for biological variability. Blood samples were excluded only if they were >6 h old before the study was conducted, and microfluidic devices were excluded due to fabrication abnormalities, such as leakage. Data analysis were performed using Graphpad Prism V7. A t-test was used.

2.10 Results and Discussion

2.10.1 Heparin Sensitivity

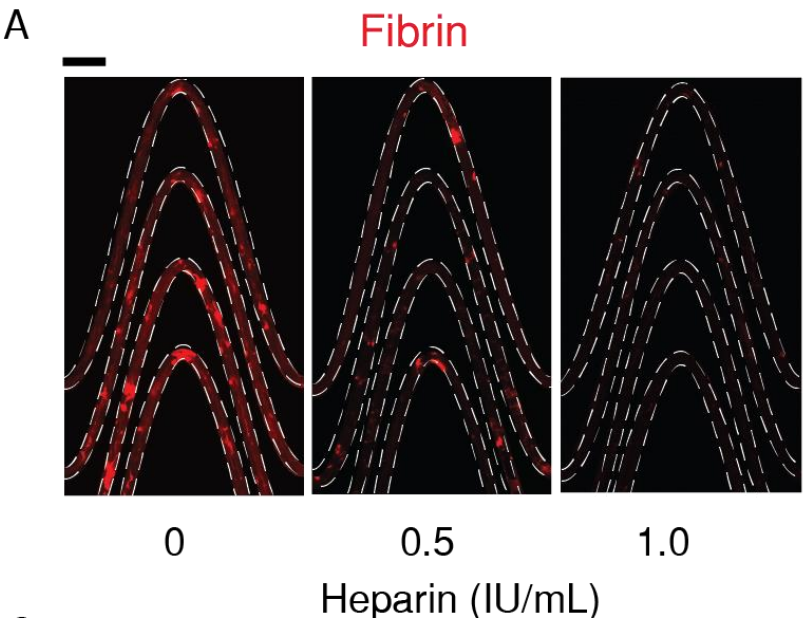

Figure 2-11. Representative fluorescent micrographs of fibrin in re-calcified citrated whole blood treated with varying heparin doses (0, 0.5, 1.0 IU/mL) after perfusion (shear gradient 935 1/s/mm) for 15 minutes (scale bar, 1mm).

When we added clinically-relevant doses (0, 0.5, 1 IU/mL) of UFH to whole blood samples fluorescently labeled for fibrin, and perfused the blood though the device while monitoring fibrin formation using fluorescent microscopy, we found a dose-dependent decrease in fibrin formation. (Fig 2-11).

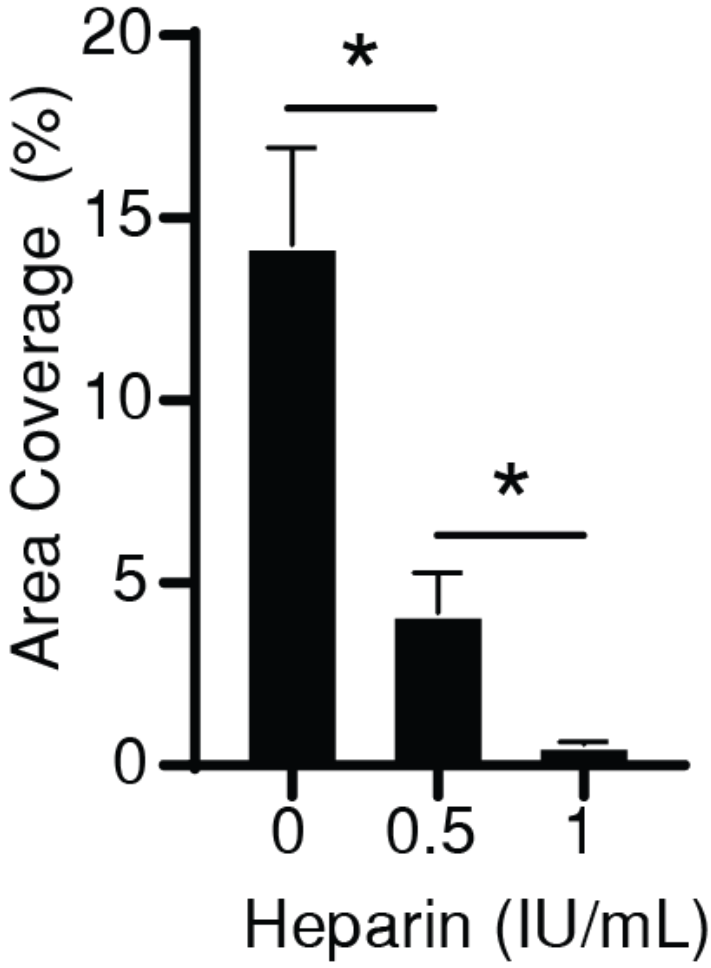

Figure 2-12. Graph showing area coverage of fibrin at a section of the tortuous region for varying heparin doses (0, 0.5, 1.0 IU/mL); (*P<0.05, unpaired t-test, s.e.m.; n=3 donors (1 replicate per experiment).

Furthermore, when we measured the images for fibrin area coverage we also found a dose-dependent decrease in fibrin formation as a function of increasing heparin dosage (Fig 2-12). These results demonstrate this device can detect differences in heparin dosage in its clinical range within healthy blood samples *in-vitro* and may be used for heparin therapy monitoring.

2.10.2 Bivalirudin Sensitivity

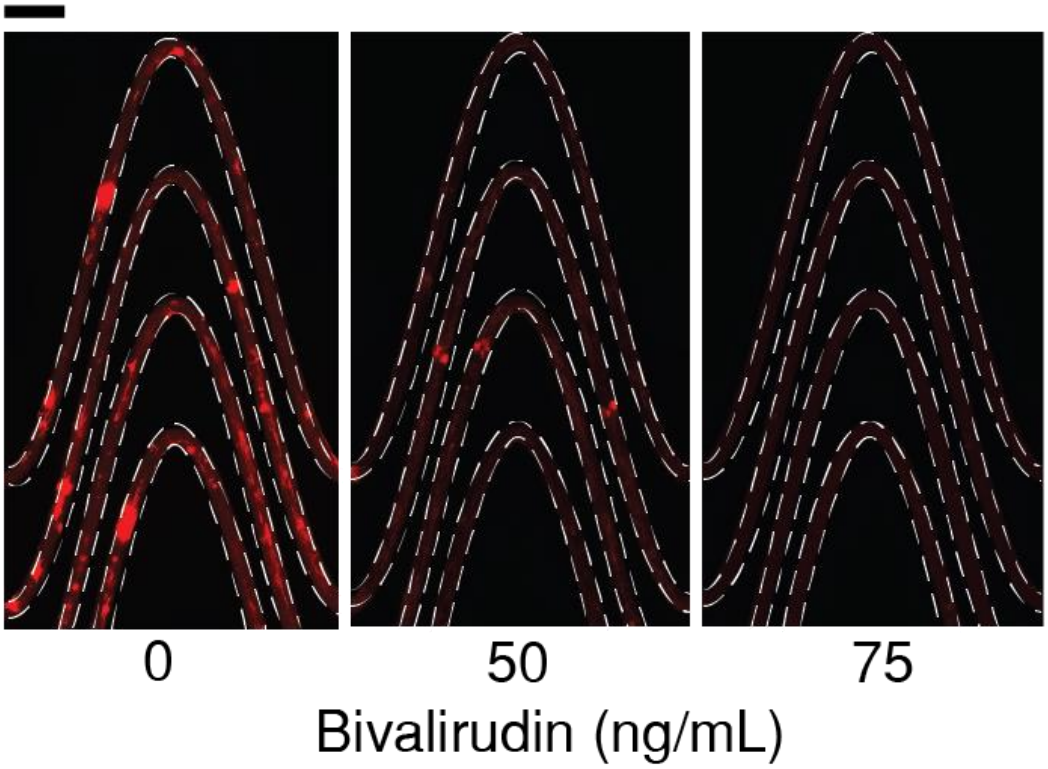

Figure 2-13. Representative fluorescent micrographs of fibrin in re-calcified citrated whole blood treated with varying bivalirudin doses (0, 50, 75 ng/mL) after perfusion (shear gradient 935 1/s/mm for 15 minutes (scale bar, 1mm).

When we followed the same methodology as described above for heparin, but instead added increasing doses of bivalirudin (0, 50, 75 ng/mL) to whole blood, we saw a dose-dependent decrease in fibrin formation (Fig 2-13).

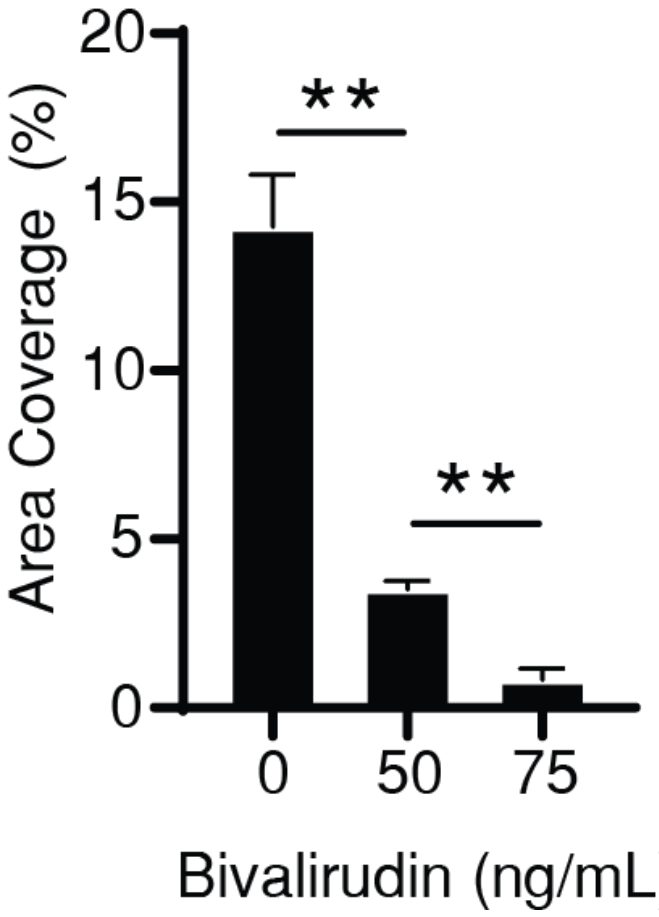

Figure 2-14. Graph showing area coverage of fibrin at a section of the tortuous region for varying bivalirudin doses (0, 50, 75 ng/mL); (**P<0.01, unpaired t-test, s.e.m.; n=3 donors (1 replicate per experiment).

Furthermore, when we measured the images for fibrin area coverage we also found a dose-dependent decrease in fibrin formation as a function of increasing bivalirudin dosage (Fig 2-14). Interestingly, our device detected nearly complete clearance of fibrin at 75ng/mL even though the therapeutic range for bivalirudin is within 0-25µg/mL, suggesting that current monitoring tools may not be detecting bleeding risk at higher bivalirudin concentrations.

2.11 In-Vitro Evaluation of Microdevice Sensitivity to Anticoagulants via Inline Pressure Measurements

These findings prompted us to develop an automated, real-time approach to monitoring anticoagulant therapy since tracking clot formation with microscopy is not realistic in a pediatric critical care setting. Therefore, we connected the device to a syringe pump, disposable pressure sensor and a display monitor as previously demonstrated (Fig 2-15) [11]. Furthermore, all of these components are conveniently part of most extracorporeal circuits and hence, currently used widely in medical settings[27].

2.11.1 Experimental Approach

2.11.1.1 Microdevice Fabrication

The stenosed-tortuous microfluidic PDMS device was fabricated using the soft lithography process as described previously in section 2.7.

2.11.1.2 Collagen Coating Process

The stenosed-tortuous microfluidic PDMS device was coated with collagen using the process as described previously in section 2.9.1.2.

2.11.1.3 Assembly of Microfluidic Device with In-line Pressure Sensor

The set up described for the anticoagulant fluorescent microscopy studies is similar to that of the in-line pressure sensor set up. The difference is that an in-line pressure sensor (PendoTECH) is sandwiched between the 10mL male luer syringe and female luer end of

tubing. Also, the in-line pressure sensor connected to a pressure display monitor which itself it connected to a laptop computer. Furthermore, the channel occlusion is measured by recording the rise in pressure over time using data acquisition and analysis software (PressureMAT, PendoTECH) installed on the PC.

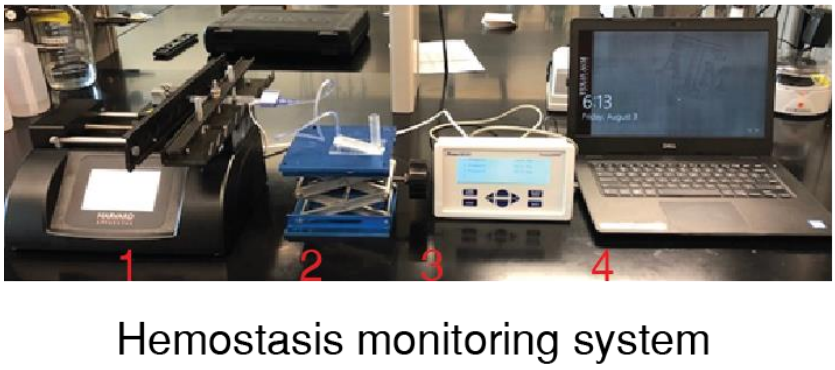

Figure 2-15. Photograph of components of tortuosity activated microfluidic thrombus and hemostasis monitoring system 1) syringe pump 2) microfluidic device 3) pressure monitor 4) laptop

2.11.1.4 Monitoring Effect of Anticoagulants on Fibrin Formation via In-Line Pressure Sensor

Healthy blood samples were collected after informed, written consent as per ethical guidelines of Institutional Review Board of Texas A&M University. Healthy donor blood was collected from non-smoking volunteers in a 3.2% 2.7mL sodium citrate vacutainers (BD). Coagulation experiments were initiated within 30 minutes after the blood draw.

The process to measure thrombus formation via in-line pressure sensor is described here. First, set the flow rate to 70 µL/min (corresponds to 1,200 1/s which is a typical arterial shear rate) on the Harvard Apparatus syringe pump. Next, open the PendoTech software

on the PC and tare the pressure display. First, load 1mL of PBS (-/-) into the reservoir and start perfusing. PBS (-\-) will have a pressure around 0.5 +/- 0.1 PSI. Once this baseline pressure is reached begin recording the pressure by selecting “Start Experiment”. Then remove 0.8mL of PBS (-/-) from the reservoir and add 1mL of fresh blood. Removing this residual PBS (-/-) prevents reduction of hematocrit. Immediately after adding blood, spike the blood with clinically relevant doses of either heparin and/or bivalirudin, then mix the sample. Wait for the blood sample to baseline around 1.6 +/- 0.2 PSI until adding 100uL/mL of 100mM calcium chloride/75mM magnesium chloride solution. After adding the recalcification solution observe for 15-20 minutes the pressure trace.

2.11.1.5 Microfluidic Clotting Time Analysis

We applied a measurement to the pressure over time readouts to serve as an automated, robust and physiologically-relevant analytical end point to be used for clinical decision making. The end point is the time it takes for the pressure to reach 2.5x baseline. We chose 2.5x because this measurement reduced the time and blood volume required for this assay, which is particularly important in the pediatric critical care setting.

2.11.1.6 Statistical Analysis

The statistical analysis used for the in-line pressure measurements as the method described in section 2.9.1.6.

2.12 Results and Discussion

2.12.1 Heparin Sensitivity

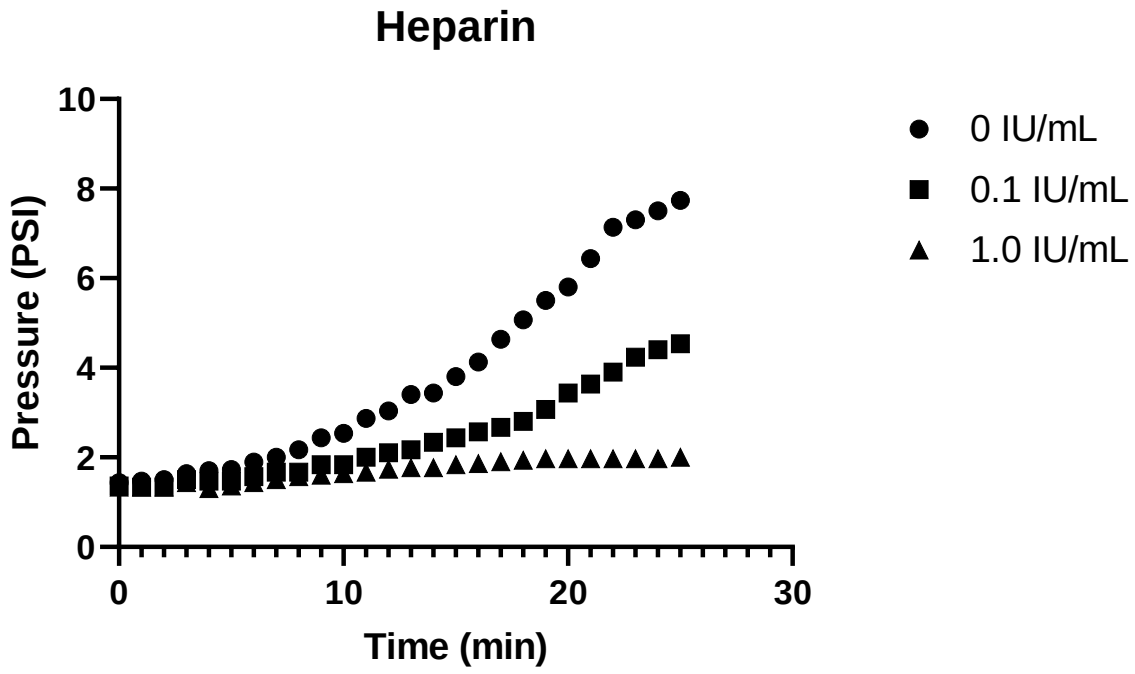

Figure 2-16. Trace of pressure measured in the device when re-calcified citrated whole blood treated with varying heparin doses (0, 0.1, 1.0 IU/mL) was perfused (shear gradient 935 1/s/mm) through horse collagen type 1 coated devices; n=3 donors (1 replicate per experiment), mean.

Using this system we can record the evolution of blood clots in real-time inside the device. Importantly, we show that as recalcified citrated whole blood is perfused and clots inside the device, the pressure increases as is typical of the dynamics of clotting in blood vessel in vivo, or in an *in vitro* hollow channel, consisting of three stages - a steady reaction time, a growth phase, and saturation [39]. However, when we added clinically relevant doses

(0, 0.1, 1.0 IU/mL) of UFH into blood, we saw that the pressure rise shifted relative to normal controls in a dose dependent manner (Fig 2-16).

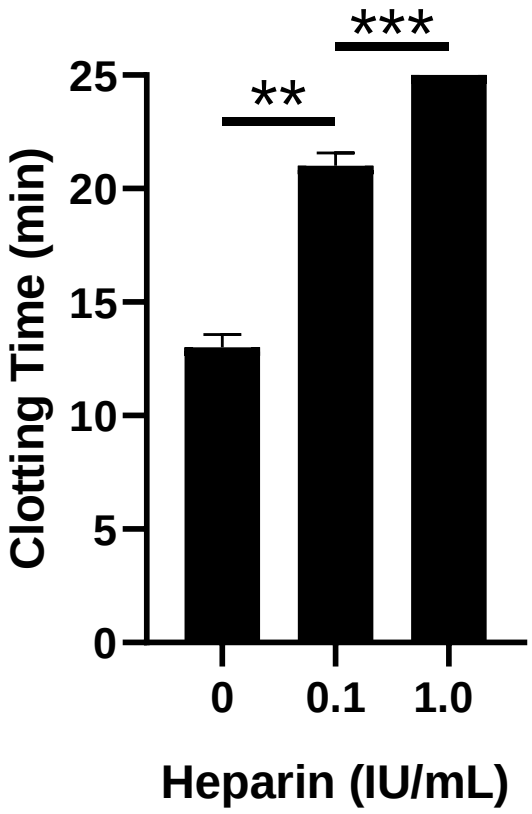

Figure 2-17. Clotting time (CT) derived from heparin pressure trace;(**P<0.01, ***P<0.001, unpaired t-test, s.e.m.; n=3 donors, 1 replicate per experiment)

Next, we developed a clotting time measurement for these pressure readouts to serve as quantitative end points in lab and clinical settings. We determined the clotting time to be a 2.5x rise in pressure from baseline because this reduced the time and blood volume required for this assay, which is particularly important in the pediatric critical care setting.

When we applied this measurement to the pressure readouts, the clotting times decreased in a dose-dependent manner for heparin. (Fig 2-17).

2.12.2 Bivalirudin Sensitivity

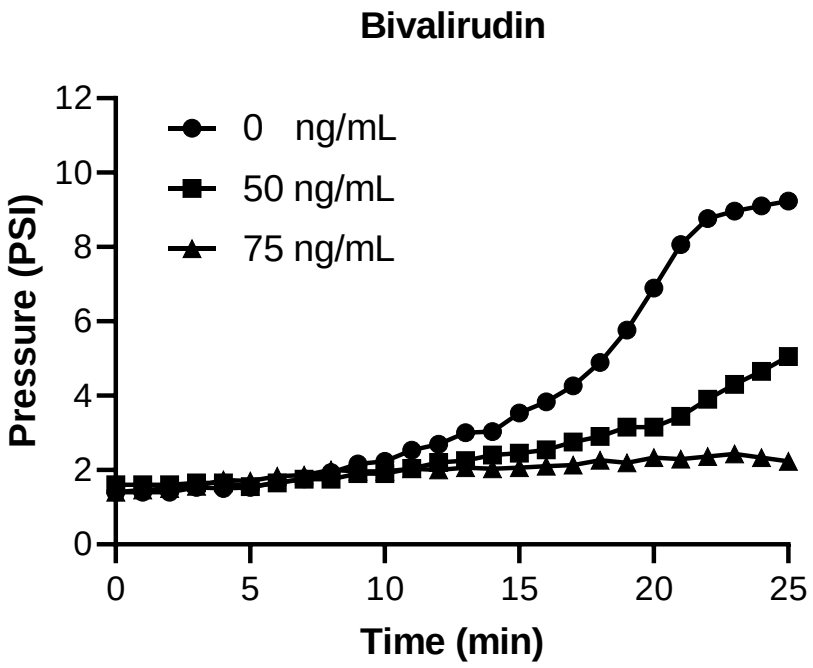

Figure 2-18. Trace of pressure measured in the device when re-calcified citrated whole blood treated with varying bivalirudin doses (0, 50, 75 ng/mL) was perfused (shear gradient 935 1/s/mm) through rat collagen type 1 coated devices; (n=3 donors, 1 replicate per experiment), mean.

We saw a similar trend when we used bivalirudin (0, 50, 75 ng/mL) instead of heparin (Fig 2-18), demonstrating that this pressure based setup can reliably detect differences in

anticoagulant dosages *in-vitro* and potentially be used for monitoring anticoagulant therapy.

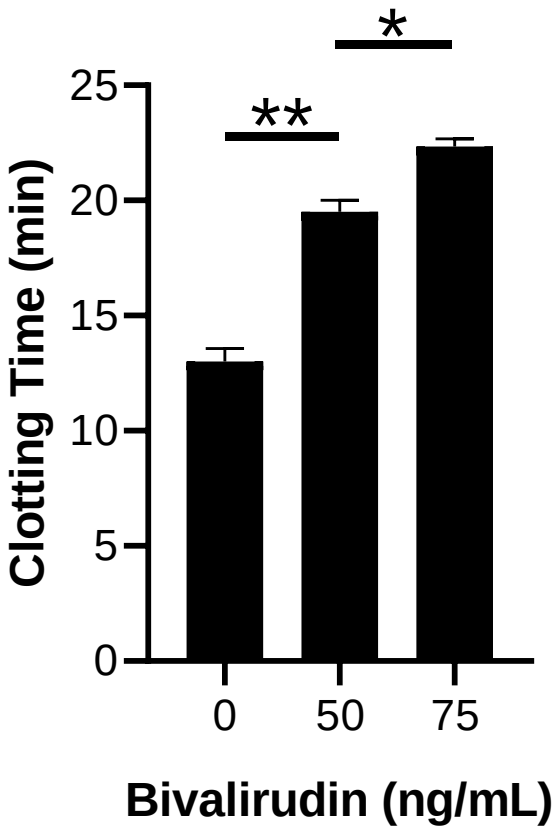

Figure 2-19. Clotting time (CT) derived from bivalirudin pressure trace; (*P<0.05, **P<0.01, unpaired t-test, s.e.m.; n=3 donors, 1 replicate per experiment)

When we applied this measurement to the pressure readouts, the clotting times decreased in a dose-dependent manner for bivalirudin. (Fig 2-19). Interestingly, we found that the overall speed of the assay can be reduced by using horse collagen type I, however; we also observed more variability with this extracellular matrix, suggesting that rat collagen type I may be a more suitable matrix for monitoring anticoagulant therapy.

2.13 *In Vitro* Platelet Function Test

As platelets are central to primary hemostasis where the final product in that process is a platelet plug, we further explored if this biomimetic device can be used to detect platelet function under stenosed flow [40]. First, we set out to determine the optimal extracellular matrix to accelerate platelet adhesion, activation, granule release, and aggregation to reduce the blood volume and time required for analysis. Second, we were interested in exploring if the microdevice is sensitive to differences in platelet count since pediatric ECLS patients are low platelet counts.

2.13.1 Experimental Approach

2.13.1.1 Microdevice Fabrication

The stenosed-tortuous microfluidic PDMS device was fabricated using the soft lithography process as described previously in section 2.7.

2.13.1.2 Procedure for Coating Different Extracellular Matrices

Collagen is an extracellular matrix protein that surrounds the endothelium of a blood vessel. When the endothelium is injured, collagen in the sub-endothelium is exposed to the blood where it acts as a platelet agonist, aiding in the activation and aggregation of platelets [38].

This section will describe the process of coating the stenosed-tortuous microfluidic device with collagen. First, the PDMS device is placed in the plasma machine and treated with

oxygen plasma (45 s, 100W) to oxidize the PDMS surface. The oxidized surface is covered with hydroxyl groups which react with chemical groups on collagen which allow for strong collagen adhesion. Immediately, after plasma treatment (within 10 minutes), collagen type 1 which either rat or horse or human is diluted to 100 µg/mL in PBS (-/-). The diluted collagen is then pushed via 1mL slip tip syringe through a 1.5 mm OD barbered connector in the inlet port of the device. Next, the collagen coated devices are placed in a petri dish and submerged in PBS (-/-) with 1mL slip tip plugs connected to the slip tip side of the 1.5 mm OD barbed connector in each port to prevent leaking and incubated in 5% CO2 for 1 hour.

2.13.1.3 Procedure for Varying Platelet Count

This section will describe the process of how to reduce or increase the platelet count in whole blood samples. As previously stated, healthy blood samples were collected after informed, written consent as per ethical guidelines of Institutional Review Board of Texas A&M University. Healthy donor blood was collected from non-smoking volunteers in a 3.2% 2.7mL sodium citrate vacutainers (BD). Complete Blood Count (CBC) measurements were taken using the Erba Diagonstics Hemavet. These readouts were taken to confirm successful platelet count manipulation.

Citrated whole blood samples were centrifuged via a two-spin process to obtain platelet-rich-plasma (PRP) [41]. First, a “soft spin” setting was executed in which whole blood was spun down for 10 min at 270g. This process separates the blood into 3 distinct layers that form based on the density of blood components. The three layers are as follows (from

top to bottom): 1) a plasma layer which consists of blood proteins 2) a buffy coat layer which consists of white blood cells and platelets, and 3) a red blood cell layer. Next, the top two layers (plasma and buffy coat) are carefully removed and placed into a 5mL Eppendorf tube. Normally from 1, 2.7mL vial of citrated whole blood at least 1.8mL of liquid comprising of both the plasma and buffy coat should be drawn. Next, the Eppendorf tube is centrifuged using a "hard spin" setting which is at 10min spin at 540g. Following the "hard spin", a pellet of platelets should be noticeable at the bottom of the Eppendorf tube. Now, to make whole blood with reduced platelet count, simply remove the supernatant from the Eppendorf tube that was spun hard without drawing up the platelet pellet and add it back to the original tube that only contains red blood cells. The resulting vial should have significantly less platelet count. On the other hand, if you want to make whole blood with 2x platelet count, then remove 1.6mL of supernatant from the Eppendorf tube, re-suspend the platelet pellet, and then add that solution of 0.2mL PRP to a fresh vial of citrated whole blood. If a 3x or 4x PC is required, then follow the above procedure with the required number of vials to reach the desired concentration.

2.13.1.4 Assembly of Microfluidic Device for In-Line Pressure Measurements

The collagen coated microfluidic device was assembled for in-line pressure measurements as previously described 2.9.1.6.

2.13.1.5 Measuring Effect of Varying Extracellular Matrices on Thrombus Formation Via In-Line Pressure Sensor

The process to measure effect of varying extracellular matrices on thrombus formation via in-line pressure sensor is similar to the procedure described previously for the anticoagulant sensitivity studies, except the microdevices have different extracellular matrices and no anticoagulant is used.

2.13.1.6 Measuring Effect of Varying Platelet Count on Thrombus Formation Via In-Line Pressure Sensor

The process to measure effect of varying extracellular matrices on thrombus formation via an in-line pressure sensor is similar to the procedure described in section 2.11.1.4, except no anticoagulant medications are added to the blood.

2.13.1.7 Statistical Analysis

The statistical analysis used for the platelet functions test are the same as the method described in section 2.9.1.6.

2.14 Results and Discussion

2.14.1 Extracellular Matrix

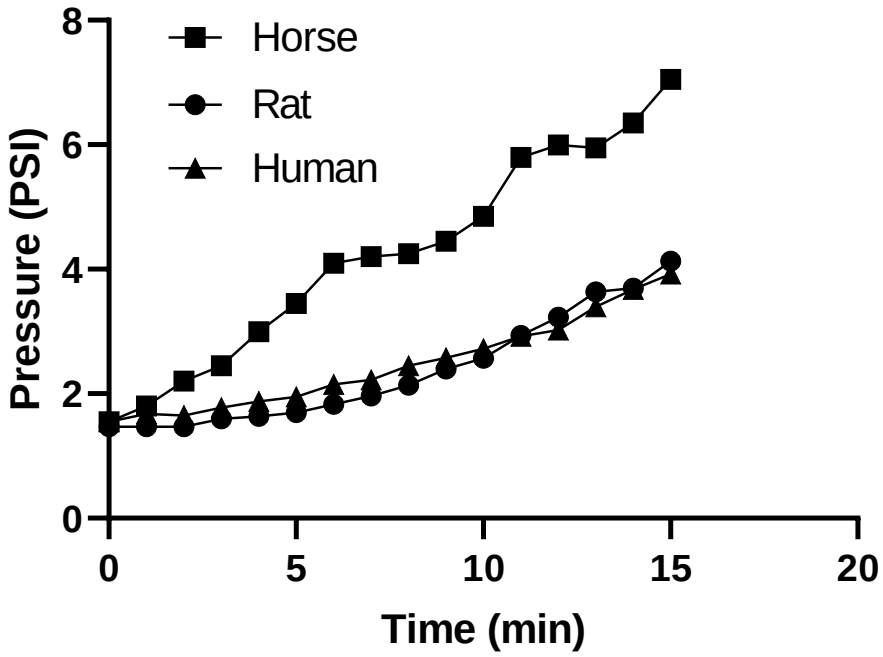

Figure 2-20. Trace of pressure measured in the device when re-calcified citrated whole blood is perfused (shear gradient 935 1/s/mm) over varying collagen type I (rat, horse, human) coated devices; (n=3 donors, 1 replicate per experiment).

First, we set out to determine the optimal platelet agonist to reduce the blood volume and time required for analysis. Therefore, we perfused recalcified whole blood through devices coated with 100 µg/mL of either rat, horse or human collagen type I and recorded and quantified clotting times. We found that the pressure trace for horse collagen type I was shifted to the left relative to rat and human collagen type I, suggesting the horse collagen type I is a more potent platelet agonist (Fig 2-20).

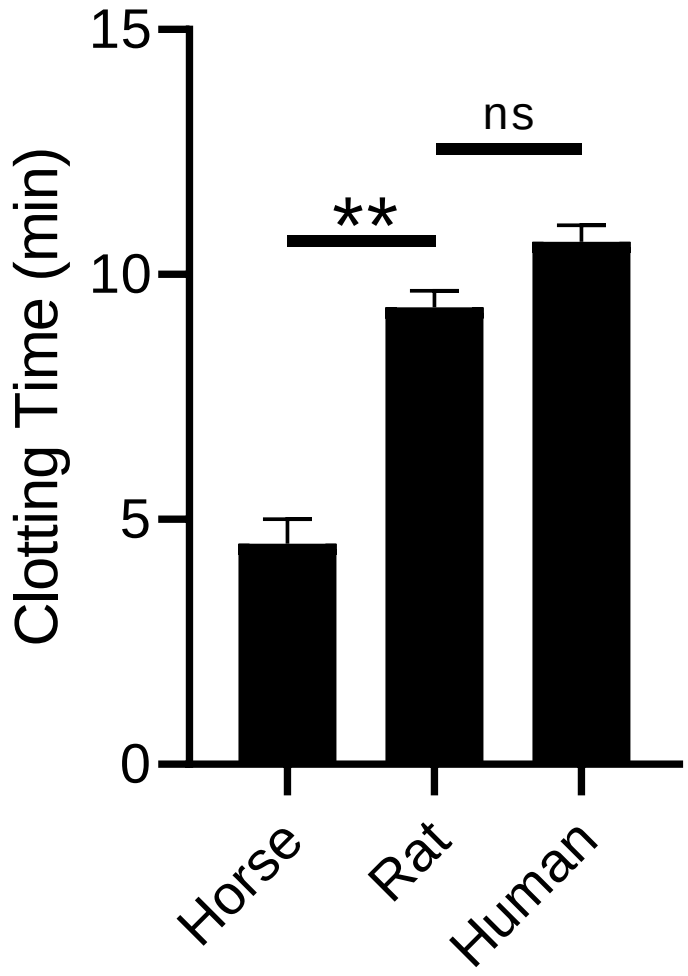

Figure 2-21. Clotting time (CT) derived from collagen type I pressure trace; (**P<0.01, unpaired t-test, s.e.m.; n=3 donors, 1 replicate per experiment).

Also, horse collagen type I had a faster clotting time compared to rat and human collagen type I (Fig 2-21), indicating that the horse collagen may be an optimal substrate to assess platelet function.

2.14.2 Platelet Count

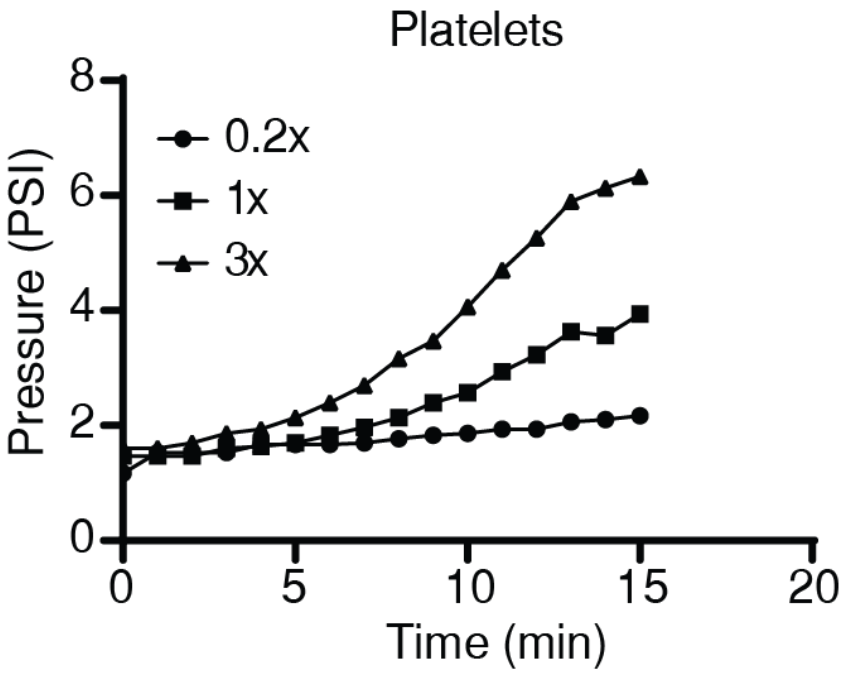

Figure 2-22. Trace of pressure measured in the device when re-calcified citrated whole blood with varying platelet count (90 x103, 385 x 103, 116 x 104 K/µL) is perfused (shear gradient 935 1/s/mm) over rat collagen type I coated devices; (n=3 donors, 1 replicate per experiment).

Next, we used rat collagen type I coated devices to analyze blood samples with varying platelet counts to explore if this device can be used to predict disorders where platelet count is low or elevated. Using a centrifuging process with whole blood we produced blood samples with 0.2x and 3x platelet counts relative to normal controls, 1x. When these samples were perfused and recorded for pressure, we observed a relative shift to the right and left for the 0.2x and 3x samples, respectively (Fig 2-22).

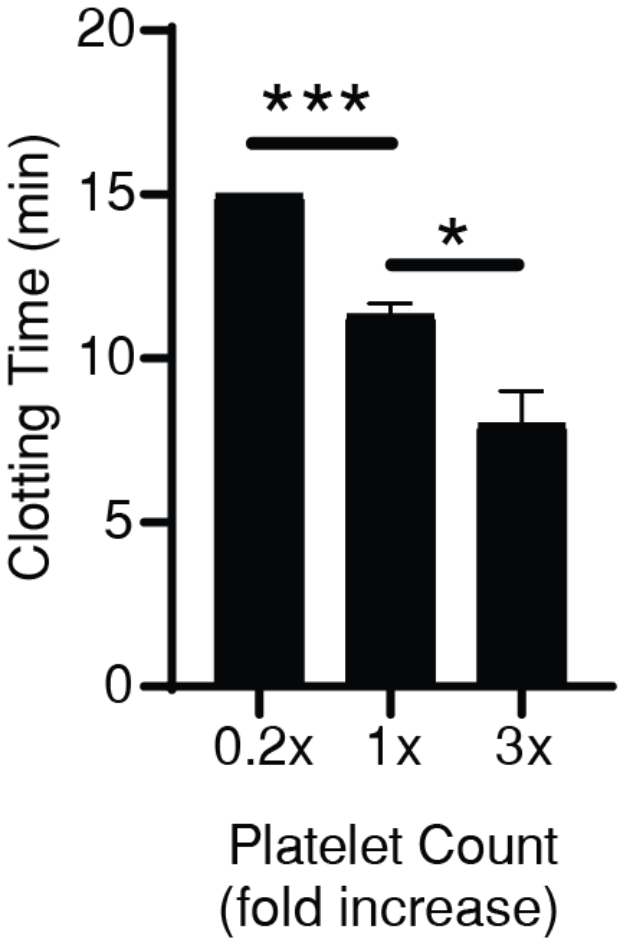

Figure 2-23. Clotting time (CT) derived from platelet count pressure trace; (*P<0.05, ***P<0.001, unpaired t-test, s.e.m.; n=3 donors, 1 replicate per experiment)

Also, when these pressure traces were measured for clotting time we observed a dose-dependent decrease in clotting time as a function of increasing platelet count (Fig 2-23). These results validate that platelets are a critical component of thrombus formation since their removal and addition to blood affected clotting dynamics. Moreover, we demonstrate that this device could potentially be used to for predicting conditions associated with platelet count.

2.15 **Platelet Function and Coagulation Factor Deficiency Analysis in Pediatric Critical Care**

Pediatric patients on ECLS typically have low platelet counts, platelet dysfunction and loss of coagulation factors [42, 43]. As a result, they are highly susceptible to bleeding despite adequate anticoagulation therapy. More concerning is the fact that current hemostasis tests that evaluate coagulation or platelet function often report positive even when bleeding risk is present. Here, we explored whether we could use this biomimetic microfluidic device to measure clotting defects in blood samples from pediatric patients on extracorporeal membrane oxygenation (Fig 2-24).

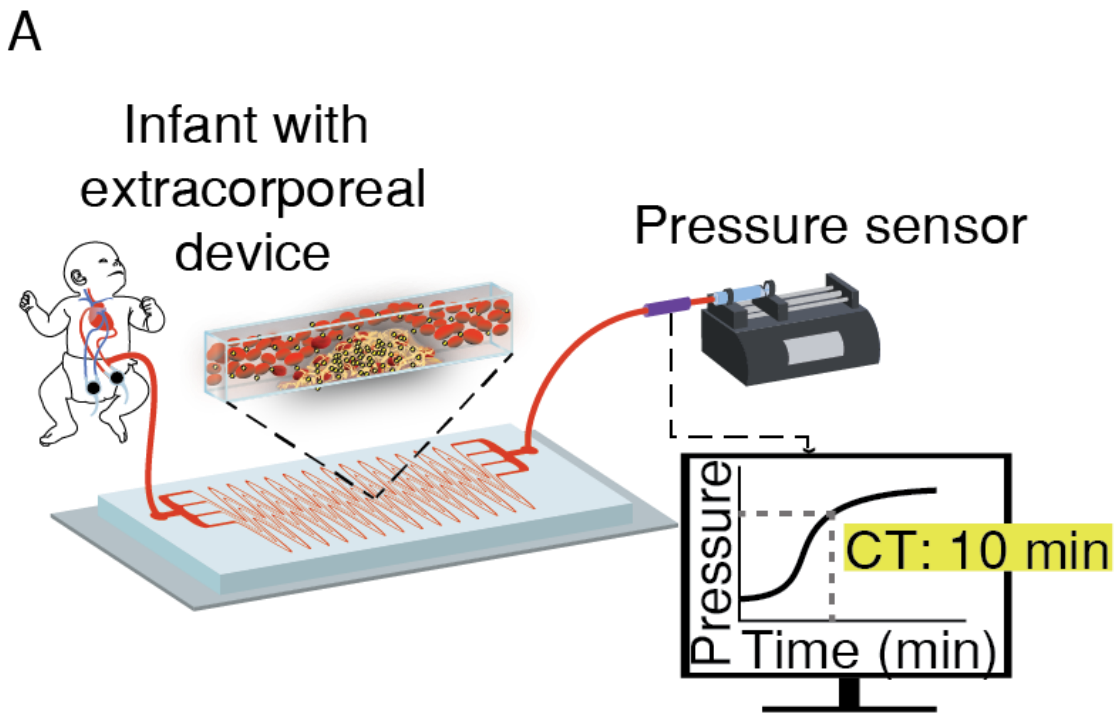

Figure 2-24. Conceptual illustration of pediatric patient with extracorporeal device connected to tortuosity-activated microfluidic thrombus and hemostasis monitoring syste

2.15.1 Experimental Approach

2.15.1.1 Pediatric Blood Samples

Pediatric blood samples were collected after informed, written consent as per ethical guidelines of Institutional Review Board of Texas Children's Hospital. Pediatric blood samples were collected in a 3.2% 2.7mL sodium citrate vacutainers (BD). Coagulation experiments were initiated within 3 hours after the blood draw.

2.15.1.2 Preparation of Collagen-Coated Microfluidic Device for In-Line Pressure Measurements

The stenosed-tortuous microfluidic PDMS device was fabricated using the soft lithography process as described previously section 2.7. The microfluidic device was coated with rat collagen type I as described previously in section 2.9. Furthermore, the microfluidic device was assembled for in-line pressure measurements as described previously in section 2.11.

2.15.1.3 Measuring Thrombus Formation in Pediatric Samples

The procedure to measure thrombus formation with pediatric blood samples with the in-line pressure measurement set up is similar to the process described in section 2.11.

2.15.1.4 Measuring Thrombus Formation in Pediatric Samples Treated with Healthy Platelets

This section will describe the process of adding healthy platelets to pediatric blood samples for in-line pressure measurements of thrombus formation. First, acquire the platelet count for the pediatric samples. Pediatric ECMO patients typically exhibit thrombocytopenia since it is known that the ECMO machine "eats" circulating platelets and other blood components. Therefore, the platelet count should be less than or about 150 K/µL.

Second, acquire the platelet count for the adult blood. The platelet count should be between 300-400 K/µL for a healthy patient. Next, spin down the adult blood samples by following the 2-step centrifugation process as previously described. Re-suspend the platelet pellet in about 0.3mL of plasma, resulting in a platelet concentration of 2.7×10^9 platelets/mL. Next, determine the amount of volume that needs to be removed from the re-suspended solution to increase the pediatric platelet concentration 2, 3, or 4 fold. For increasing pediatric platelets concentration to higher folds it will be necessary to combine platelets from multiple vials to ensure enough platelets are available to increase the platelet concentration that amount. Also, pediatric platelet concentrations are reported as being normalized to adult platelet concentrations. For instance, the adult platelet count was 350 K/µL and the pediatric platelet counts were 176, 352 and 528 K/µL, respectively. After normalizing to the adult platelet count these values become 0.5x. 1.0x and 1.5x. After the samples are prepared, load them into the reservoir of the microfluidic device, and acquire pressure measurement of thrombus formation as previously described.

If time-lapse fluorescent images of platelets adhesion to the collagen substrate are required, then it will be necessary to increase the amount of CD-41 FITC antibody accordingly. For instance, the normal amount of antibody added is 10µL/mL, however if the platelet concentration is increase 2, 3, or 4 fold then the amount dose of antibody needs to reflect that change in platelet amount to allow accurate comparison of results.

2.15.1.5 Quantification of Platelet Area Coverage

The image processing method described in section 2.9 to quantify fibrin area coverage was applied for platelets.

2.15.1.6 Statistical Analysis

The statistical analysis used for the platelet functions test are the same as the method described in section 2.9.1.6.

2.16 Results and Discussion

2.16.1 Whole Blood Monitoring of Pediatric ECMO Samples

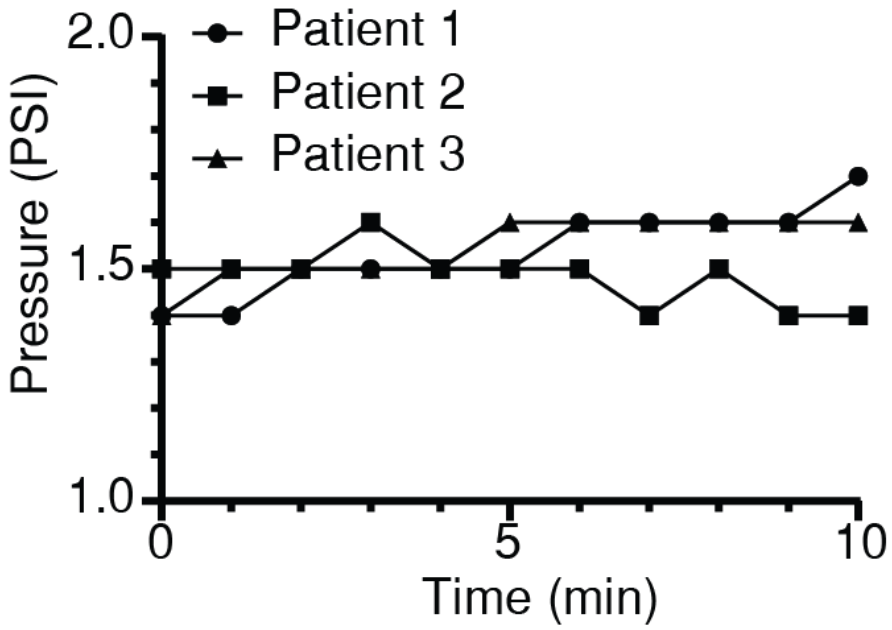

Figure 2-25. Trace of pressure measured in the device when re-calcified citrated pediatric ECMO whole blood is perfused (shear gradient 935 1/s/mm) over rat collagen type I coated devices; (n=3 donors, 1 replicate per experiment**)**

Interestingly, when we perfused the device with blood from pediatric ECMO patients, we did not observe any clotting for the entire duration of the experiment in all four subjects (Fig 2-25). These findings show that this microfluidic device can recapitulate the susceptibility to bleeding *in vitro* (that is, failure to form clot normally within flow blood in vivo). Furthermore, we demonstrate that analysis within these blood samples takes less than 15 minutes to complete and requires less than 1mL of blood sample.

2.16.2 Whole Blood Monitoring of Pediatric ECMO Samples Spiked with Healthy Platelets

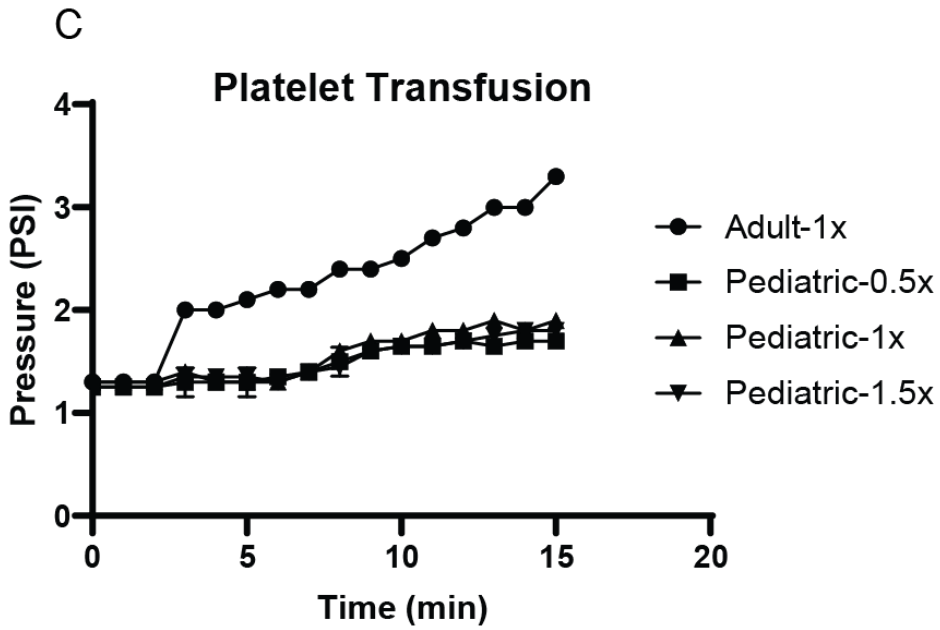

Figure 2-26. Trace of pressure measured in the device when re-calcified citrated pediatric ECMO whole blood spiked with healthy platelets (0.5x, 1.0x, and 1.5x relative to adult control) is perfused (shear gradient 935 1/s/mm) over rat collagen type I coated devices; (n=1 donors, 1 replicate per experiment).

Next, we then performed a platelet transfusion *in vitro* since transfusions are commonly administered to pediatric ECMO patients to reduce bleeding risk [44]. We found that when we added increasing amount of healthy platelets (0.5x, 1.0x, and 1.5 x relative to adult control) to the pediatric blood microchannel occlusion was not restored (Fig 2-26).

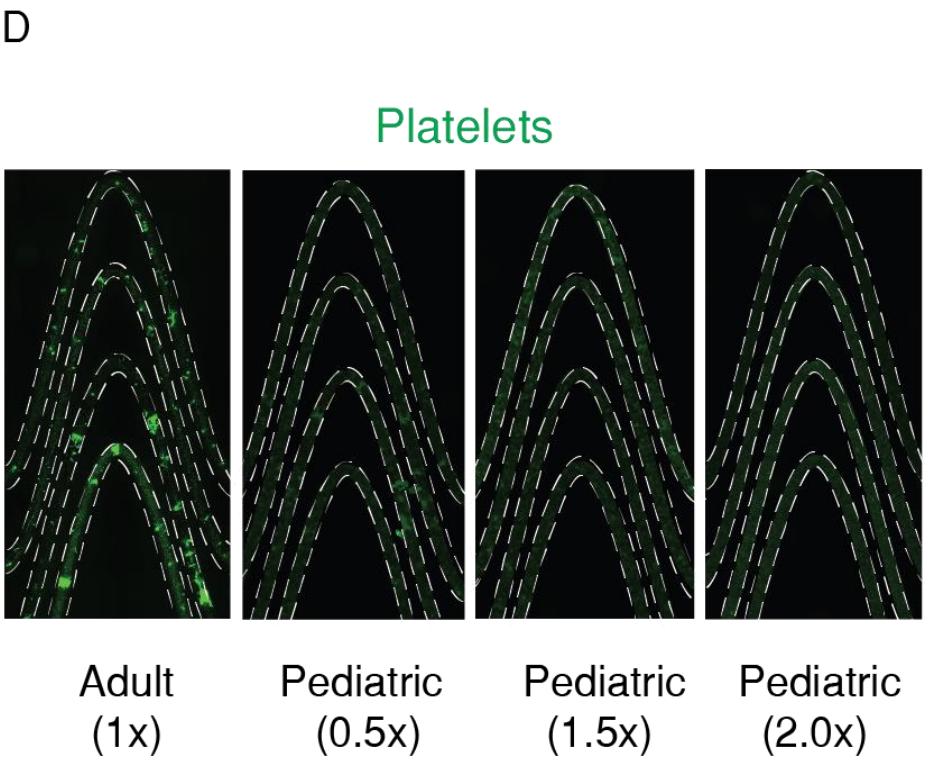

Figure 2-27. Representative fluorescent micrographs comparing platelet adhesion in pediatric ECMO whole blood sample spiked with healthy platelets (0.5x, 1.0x, and 1.5x relative to adult control) and healthy controls after perfusion (shear gradient 935 1/s/mm for 15 minutes (scale bar, 1mm).

Moreover, we show poor platelet adhesion even when healthy platelets are added, suggesting that these patients have a coagulation factor deficiency (Fig 2-27). We next explored if clotting in this device can restored with the addition of von willebrand factor (VWF) which is a coagulation factor that is commonly damaged and reduced in ECMO patients [45, 46]. To test this, we will add recombinant VWF (Vonvendi) to pediatric ECMO blood samples and determine if platelet adhesion is restored. Table 1-1 provides complete blood count results from all four pediatric ECMO patients.

Pediatric Patient	Hgb (11.5-15.5 g/dl)	Hct (35-45%)	Plt (150-450)
1	9.8	29.0	125
2	11.4	35.0	131
3	12.4	38.1	153
4	11.5	35.2	176

Table 1-1. Complete Blood Count showing hemoglobin, hematocrit and platelets for pediatric ECMO patients.

3. CONCLUSION

3.1 Novelty of Biomimetic Tortuous Blood Vessel Microdevice

The tortuosity-activated microfluidic thrombus and hemostasis monitoring device described here provides several potential advantages over other tests used to monitor hemostasis. First, due to the presence of whole blood flow and shear-gradients induced by the stenosed and tortuous architecture of the device, clot formation occurs under near-pathophysiological conditions and includes complex blood rheology that is critical to thrombosis. Another major advantage of this biomimetic device is that when connected to a pressure sensor, we can record clotting within the device in real-time. Using this system, we also were able to identify a clotting time measurement to provide an automated, robust and physiologically-relevant analytical end point. This clotting time showed sensitivity to heparin and bivalirudin therapy *in vitro*, platelet adhesion to different collagen matrices, and varying platelet concentration, making this device well suited to explore novel anti-coagulants and evaluate platelet function. Importantly, using this measurement, we required <3-fold rise in pressure drop to reliably measure hemostasis, which minimizes the time and blood samples that are required to carry out these studies. Hence, the efficiency of this device makes it well suited for applications in pediatrics where it is critical to consume less than 1mL of blood sample volume. As such we demonstrated that this system can detect bleeding rick pediatric ECMO patients, which is often missed with current hemostasis monitoring tools. Finally, we have also gained some interesting new

insights into the biophysical process of thrombus formation through use of this device. For instance, we integrated the shear gradients induced by stenosis to tortuosity-driven gradients in the microdevice and found that blood clots formed more rapidly. The cause of this response is unknown, but it is likely due to the activation of clotting factors, platelets and/or immune cells via fluid dynamic-dependent mechanical signaling pathways that remain to be defined. In any case, this device may be useful for personalized diagnostics and for real-time surveillance of antithrombotic therapy in the clinic.

REFERENCES

1. Adachi, I., et al., *Management of Hemostasis for Pediatric Patients on Ventricular-Assist Devices.* Semin Thromb Hemost, 2017.
2. Ryerson, L.M. and L.L. Lequier, *Anticoagulation Management and Monitoring during Pediatric Extracorporeal Life Support: A Review of Current Issues.* Front Pediatr, 2016. **4**: p. 67.
3. Saini, A. and P.C. Spinella, *Management of anticoagulation and hemostasis for pediatric extracorporeal membrane oxygenation.* Clin Lab Med, 2014. **34**(3): p. 655-73.
4. Dalton, H.J., et al., *Factors Associated with Bleeding and Thrombosis in Children Receiving Extracorporeal Membrane Oxygenation.* Am J Respir Crit Care Med, 2017. **196**(6): p. 762-771.
5. Baird, C.W., et al., *Anticoagulation and pediatric extracorporeal membrane oxygenation: impact of activated clotting time and heparin dose on survival.* Ann Thorac Surg, 2007. **83**(3): p. 912-9; discussion 919-20.
6. Kuhle, S., et al., *Lack of correlation between heparin dose and standard clinical monitoring tests in treatment with unfractionated heparin in critically III children*. Vol. 92. 2007. 554-7.
7. Kostousov, V., et al., *The influence of free hemoglobin and bilirubin on heparin monitoring by activated partial thromboplastin time and anti-Xa assay.* Arch Pathol Lab Med, 2014. **138**(11): p. 1503-6.
8. Fogelson, A.L. and N. Tania, *Coagulation under flow: the influence of flow-mediated transport on the initiation and inhibition of coagulation.* Pathophysiol Haemost Thromb, 2005. **34**(2-3): p. 91-108.
9. Nesbitt, W.S., et al., *A shear gradient-dependent platelet aggregation mechanism drives thrombus formation.* Nat Med, 2009. **15**(6): p. 665-73.
10. Westein, E., et al., *Atherosclerotic geometries exacerbate pathological thrombus formation poststenosis in a von Willebrand factor-dependent manner.* Proc Natl Acad Sci U S A, 2013. **110**(4): p. 1357-62.
11. Jain, A., et al., *A shear gradient-activated microfluidic device for automated monitoring of whole blood haemostasis and platelet function.* Nat Commun, 2016. **7**: p. 10176.
12. Liu, Q., D. Mirc, and B.M. Fu, *Mechanical mechanisms of thrombosis in intact bent microvessels of rat mesentery.* J Biomech, 2008. **41**(12): p. 2726-34.
13. Chesnutt, J.K. and H.C. Han, *Tortuosity triggers platelet activation and thrombus formation in microvessels.* J Biomech Eng, 2011. **133**(12): p. 121004.
14. *http://practical-haemostasis.com/Miscellaneous/Miscellaneous%20Tests/act.html.*
15. Basu, D., et al., *A prospective study of the value of monitoring heparin treatment with the activated partial thromboplastin time.* N Engl J Med, 1972. **287**(7): p. 324-7.
16. *http://practical-haemostasis.com/Miscellaneous/Miscellaneous%20Tests/anti_xa_assays.html.*

17. O'Meara, L.C., et al., *Anti-xa directed protocol for anticoagulation management in children supported with extracorporeal membrane oxygenation.* ASAIO J, 2015. **61**(3): p. 339-44.
18. Ganter, M.T. and C.K. Hofer, *Coagulation monitoring: current techniques and clinical use of viscoelastic point-of-care coagulation devices.* Anesth Analg, 2008. **106**(5): p. 1366-75.
19. Northrop, M.S., et al., *The use of an extracorporeal membrane oxygenation anticoagulation laboratory protocol is associated with decreased blood product use, decreased hemorrhagic complications, and increased circuit life.* Pediatr Crit Care Med, 2015. **16**(1): p. 66-74.
20. *http://practical-haemostasis.com/Platelets/platelet_function_testing_lta.html.*
21. Gresele, P., et al., *Diagnosis of suspected inherited platelet function disorders: results of a worldwide survey.* J Thromb Haemost, 2014. **12**(9): p. 1562-9.
22. *http://practical-haemostasis.com/Platelets/platelet_function_testing_pfa100.html.*
23. *http://www.accriva.com/uploads/literature/mvn0005_verifynow_pocket_guide_01.pdf.*
24. *https://www.haemonetics.com/~/media/Sharepoint/Devices/TEG/Marketing/Brochures/TEG_PlateletMapping/COL-PP-000196-US_TEG_Plateletmapping_Assay%20pdf.ashx.*
25. Hosokawa, K., et al., *A novel automated microchip flow-chamber system to quantitatively evaluate thrombus formation and antithrombotic agents under blood flow conditions.* J Thromb Haemost, 2011. **9**(10): p. 2029-37.
26. *https://www.t-tas.info/products/pl-chip-for-t-tas-01/.*
27. *https://www.t-tas.info/pub/.*
28. Cho, Y.I. and K.R. Kensey, *Effects of the non-Newtonian viscosity of blood on flows in a diseased arterial vessel. Part 1: Steady flows.* Biorheology, 1991. **28**(3-4): p. 241-62.
29. Duffy, D.C., et al., *Rapid Prototyping of Microfluidic Systems in Poly(dimethylsiloxane).* Anal Chem, 1998. **70**(23): p. 4974-84.
30. Sia, S.K. and G.M. Whitesides, *Microfluidic devices fabricated in poly(dimethylsiloxane) for biological studies.* Electrophoresis, 2003. **24**(21): p. 3563-76.
31. *http://microchem.com/pdf/SU-82000DataSheet2025thru2075Ver4.pdf*.
32. Sanfilippo, F., et al., *Bivalirudin for Alternative Anticoagulation in Extracorporeal Membrane Oxygenation: A Systematic Review*, in *J Intensive Care Med*. 2016.
33. Nagle, E.L., et al., *Bivalirudin in pediatric patients maintained on extracorporeal life support.* Pediatr Crit Care Med, 2013. **14**(4): p. e182-8.
34. Buck, M.L., *Bivalirudin as an Alternative to Heparin for Anticoagulation in Infants and Children.* The journal of pediatric pharmacology and therapeutics : JPPT : the official journal of PPAG, 2015. **20**(6): p. 408-417.

35. Koster, A., et al., *Monitoring of bivalirudin anticoagulation during and after cardiopulmonary bypass using an ecarin-activated TEG system.* J Card Surg, 2008. **23**(4): p. 321-3.
36. Casserly, I.P., et al., *Point-of-care ecarin clotting time versus activated clotting time in correlation with bivalirudin concentration.* Thromb Res, 2004. **113**(2): p. 115-21.
37. Carroll, R.C., et al., *Measurement of patients' bivalirudin plasma levels by a thrombelastograph ecarin clotting time assay: a comparison to a standard activated clotting time.* Anesth Analg, 2006. **102**(5): p. 1316-9.
38. Neeves, K.B., et al., *Sources of variability in platelet accumulation on type 1 fibrillar collagen in microfluidic flow assays.* PLoS One, 2013. **8**(1): p. e54680.
39. Casa, L.D., D.H. Deaton, and D.N. Ku, *Role of high shear rate in thrombosis.* J Vasc Surg, 2015. **61**(4): p. 1068-80.
40. Jackson, S.P., *The growing complexity of platelet aggregation.* Blood, 2007. **109**(12): p. 5087-95.
41. Dhurat, R. and M. Sukesh, *Principles and Methods of Preparation of Platelet-Rich Plasma: A Review and Author's Perspective.* J Cutan Aesthet Surg, 2014. **7**(4): p. 189-97.
42. Stallion, A., et al., *The significant relationship between platelet count and haemorrhagic complications on ECMO.* Perfusion, 1994. **9**(4): p. 265-9.
43. Tauber, H., et al., *Extracorporeal membrane oxygenation induces short-term loss of high-molecular-weight von Willebrand factor multimers.* Anesth Analg, 2015. **120**(4): p. 730-6.
44. Kim, H.S. and S. Park, *Blood Transfusion Strategies in Patients Undergoing Extracorporeal Membrane Oxygenation.* Korean J Crit Care Med, 2017. **32**(1): p. 22-28.
45. Jones, M.B., et al., *Acquired von Willebrand Syndrome: An Under-Recognized Cause of Major Bleeding in the Cardiac Intensive Care Unit.* World J Pediatr Congenit Heart Surg, 2016. **7**(6): p. 711-716.
46. Geisen, U., et al., *Platelet Secretion Defects and Acquired von Willebrand Syndrome in Patients With Ventricular Assist Devices.* J Am Heart Assoc, 2018. **7**(2).

APPENDIX A

FLOURESCENT IMAGE QUANTIFICATION SCRIPT

```
clc; clear all; clf;
close all;
fname = 'R:\BMEN\David-Luna\Pediatric Pressure Sensor\Pediatric
Study\Patient 4 (2.19.19)\Pediatric Flourescence\';

% tiffname = strcat(fname,'PO-4-P-05-AV-0-7500.tif');
% tiffname = strcat(fname,'PO-3-P-15-VV-0-7500.tif');
% tiffname = strcat(fname,'PO-3-P-15-VV-0-7500.tif');
% tiffname = strcat(fname,'PO-2-P-15-VV-0-7500.tif');
tiffname = strcat(fname,'3.9.19_heparin_control_plts_s1.ome.tiff');

thresh = 0.07;

info = imfinfo (tiffname);
nframes = numel(info);

m = info(1).Width;
n = info(1).Height;

tot_area = m*n

nframes = 1

for i = 1:nframes
    Istack = imread(tiffname,i);
    size(Istack);
    Istack = Istack(:,:);
    Check1 = Istack(:);
    M = (mode(Check1))
    Ma = max(Istack(:))
    Mi = min(Istack(:))
    Istack = Istack;
    Imask = imbinarize(Istack,thresh);
    BrightArea = bwarea(Imask)
    Imareafraction = 100*bwarea(Imask)/tot_area
end
```

.

APPENDIX B

PRESSURE MONITORING MEASUREMENT

```
clc
clear all

filename = "R:\BMEN\David-Luna\Pediatric Pressure Sensor\Platelet
Transfusion\2.21.19\experiment 232 (2.21.19).csv"; % THIS IS THE
PATHNAME OF THE FILE

%-------------------HOW TO COPY FILE PATH-------------------
%   1. Press down the shift key. 2. Right click on the file yo want to
%   analyze. 3. Select "Copy as path". 4. Paste it in the filename
field.
%   Make sure that there is only one set of quotes ("").
%------------------------------------------------------------

M1 = csvread(filename,3,2);
M2 = -M1(:,1);

l2=length(M2);

M3=M2(2:l2,1);

l3=l2-1;

for i=1:floor(l3/4)
    M4(i+1,1)=M3(4*i);
end

M4(1,1)=M2(1,1);
M4
```